AIMERG: a new Asian precipitation dataset (0.1°/half-hourly, 2000-2015) by calibrating GPM IMERG at daily scale using APHRODITE

Ziqiang Ma[1], Jintao Xu[2], Siyu Zhu[1], Jun Yang[3], Guoqiang Tang[4,5], Yuanjian Yang[6], Zhou Shi[2], Yang Hong[1,7]

[1]*Institute of Remote Sensing and Geographical Information Systems, School of Earth and Space Sciences, Peking University, Beijing, 100871, China*

[2]*Institute of Agricultural Remote Sensing and Information Technology Application, College of Environmental and Resource Sciences, Zhejiang University, Hangzhou, 310058, China*

[3]*National Satellite Meteorological Centre, China Meteorological Administration, Beijing, 100081, China*

[4]*University of Saskatchewan Coldwater Lab, Canmore, Alberta, Canada, T1W 3G1*

[5]*Centre for Hydrology, University of Saskatchewan, Saskatoon, Saskatchewan, Canada, S7N 1K2*

[6]*School of Atmospheric Physics, Nanjing University of Information Science and Technology, Nanjing 210044, China*

[7]*School of Civil Engineering and Environmental Science, University of Oklahoma, Norman, OK, 73019, United States*

Correspondences: Ziqiang Ma (ziqma@pku.edu.cn); Prof. Yang Hong (yanghong@ou.edu)

AIMERG: a new Asian precipitation dataset (0.1°/half-hourly, 2000-2015) by calibrating GPM IMERG at daily scale using APHRODITE

Highlights

- **A new effective daily calibration approach, DSTDCA, for improving GPM IMERG**
- **A new AIMERG precipitation data (0.1°/half-hourly, 2000-2015, Asia) is provided**
- **Bias of AIMERG is significantly improved compared with that of IMERG**
- **APHRODITE is more suitable than GPCC in anchoring IMERG over the Asia**

Abstract

Precipitation estimates with fine quality and spatio-temporal resolutions play significant roles in understanding the global and regional cycles of water, carbon and energy. Satellite-based precipitation products are capable of detecting spatial patterns and temporal variations of precipitation at fine resolutions, which is particularly useful over poorly gauged regions. However, satellite-based precipitation products are the indirect estimates of precipitation, inherently containing regional and seasonal systematic biases and random errors. In this study, focusing on the potential drawbacks in generating Integrated Multi-satellitE Retrievals for Global Precipitation Measurement (IMERG) and its recently updated retrospective IMERG in the Tropical Rainfall Measuring Mission (TRMM) era (finished in July, 2019), which were only calibrated at monthly scale using ground observations, Global Precipitation Climatology Centre (GPCC, 1.0°/Monthly), we aim to propose a new calibration algorithm for IMERG at daily scale, and to provide a new AIMERG precipitation dataset (0.1°/ half-hourly, 2000-2015, Asia) with better quality, calibrated by Asian Precipitation Highly Resolved Observational Data Integration (APHRODITE, 0.25°/Daily) at the daily scale for the Asian applications. And the main conclusions include but not limited to: (1) the proposed daily calibration algorithm (Daily Spatio-Temporal Disaggregation Calibration Algorithm, DSTDCA) is effective in considering the advantages from both satellite-based precipitation estimates and the ground observations; (2) AIMERG performs better than IMERG at different spatio-temporal scales, in terms of both systematic biases and random errors, over the China Mainland; and (3) APHRODITE demonstrates significant advantages than GPCC

in calibrating the IMERG, especially over the mountainous regions with complex terrain, e.g., the Tibetan Plateau. Additionally, results of this study suggest that it is a promising and applicable daily calibration algorithm for GPM in generating the future IMERG in either operational scheme or retrospective manner.

The AIMERG data record (0.1°/half-hourly, 2000-2015, Asia) is freely available at http://argi-basic.hihanlin.com:8000/d/d925fecf60/. Additionally, the AIMERG data is also freely accessible at https://doi.org/10.5281/zenodo.3609352 (for the period from 2000 to 2008) (Ma et al., 2020a) and http://doi.org/10.5281/zenodo.3609507 (for the period from 2009 to 2015) (Ma et al., 2020b).

Keywords: Precipitation; IMERG; APHRODITE; Calibration; Daily scale; Asia;

1. Introduction

Precipitation is among the most essential hydroclimatic factors, and also most difficult to estimate due to its great small-scale variabilities (Yatagai et al., 2012; Huffman et al., 2019a). High spatio-temporal resolution precipitation dataset with fine quality is essential for various scientific and operational applications, including but not limited to driving the hydrological models, and supporting the predictions of droughts and floods (Beck et al., 2017, 2018). There are mainly two principal approaches for measuring the global precipitation: ground-based gauge observing, and satellite-based remote sensing, which resulting in three mainstreams of global precipitation products, namely gauge analysis precipitation data, satellite-based only precipitation estimates, and satellite-gauge combined precipitation products, based on the consideration that ground-based gauge data are clearly important for anchoring the satellite estimates (Huffman et al., 2007, 2019a).

In recent years**,** a large number of quasi-global satellite precipitation products with various temporal and spatial resolutions have been developed and released to the public, such as the PMW-based CPC Morphing technique (CMORPH) (hereafter, for Acronyms, see the Appendix) (Joyce et al., 2004), and IR-based PERSIANN (Sorooshian et al., 2000) and PERSIANN-CCS (Hong et al., 2004). As the milestone in the satellite-based precipitation measurement process, the TRMM and its successor GPM developed a flexible framework for generating the most popular precipitation products, TMPA (1998-present, 0.25°/3 hourly) and IMERG (2014-present, 0.1°/half-hourly), as well as the retrospective IMERG (2000-present, 0.1°/half-hourly) from GPM era to TRMM era, which aimed at intercalibrating, merging, and interpolating all MW estimates of the GPM constellation, IR estimates, and gauge observations (Huffman et al., 2019b). The “Final run” version of IMERG (hereafter refer to IMERG), incorporating the monthly gauge analysis, provides the state-of-the-art precipitation estimate with finest spatio-temporal resolutions so far, while it still contains large uncertainties, e.g., greatly overestimating the precipitation, at daily and hourly scales from regions to regions, especially over the mountainous areas, such as the Tibetan Plateau, China (Tang et al., 2016; Lu et al., 2019; Xu et al., 2019), which is greatly potentially resulted by the calibration procedures in the process of generating the IMERG. Currently, the IMERG product (following the gauge correction method of TMPA approach) (Huffman et al., 2007) has been produced by anchoring the multi-satellite-only precipitation estimates using the monthly analysis Satellite-Gauge product (1.0°/monthly, 1979 to the present, delayed by about 3 months) from the GPCC (Adler et al., 2003, 2018), therefore, the IMERG performed better at monthly and annul scales than those at finer temporal scales (e.g., daily, hourly).

Satellite-based precipitation products have significant advantages in detecting the variations of precipitation at fine spatio-temporal resolutions, especially over the poorly gauged regions. However, as the indirect estimates of precipitation, satellite-based precipitation products are inherently containing regional, seasonal, and diurnal systematic biases and random errors (Ebert et al., 2007), which could be effectively alleviated by anchoring the satellite-only precipitation products using gauge-based observations (Huffman et al., 2007). Therefore, great efforts have been taken on exploring the calibrations on the satellite-only precipitation estimates using gauge analysis. Historically, GPCP has provided the lion's share of the early efforts in the process of developing calibration algorithms for the satellite-only precipitation estimates in generating SG products (2.5°/monthly). For instance, to correct the bias of the multi-satellite only estimates (mainly based on PMW and IR data) on a regional scale, the multi-satellite estimate was firstly multiplied by the ratio of the large-scale (with moving window size 5 × 5) average gauge analysis to the large-scale average of the multi-satellite estimate, and then the SG estimate was finally derived by combining the gauge-adjusted multi-satellite estimate and the gauge analysis with inverse-error-variance weighting (Huffman et al., 1997; Adler et 2003; Adler 2018). Recently, a two-step strategy was proposed to remove the bias inherent in the multi-satellite only precipitation estimates using

PDF matching method and to combine the bias-corrected estimates with the gauge analyses using OI algorithm (Xie and Xiong, 2011; Shen et al., 2014). And a similar improved PDF algorithm was applied to generate the GSMaP data, which was adjusted at the daily scale by the gauge analysis (0.5°/daily) from the CPC (Mega et al., 2014). While GPM IMERG adjusted the multi-satellite precipitation estimates (0.1°/half hourly) at the monthly scale using the ratios between the original monthly multi-satellite-only and the monthly satellite-gauge data, in combination with the original monthly multi-satellite-only and GPCC (1.0°), in the month (Huffman et al., 2019a). There is still much room for exploring the improved algorithms for calibrating the multi-satellite-only precipitation estimates at finer spatiotemporal scales, e. g, 0.25°/daily, which is also one of the next vital focuses by the GPM (Huffman et al., 2019a).

As for anchoring the satellite precipitation estimates, the quality and spatio-temporal resolutions of the gauge analysis precipitation data are the key factors. Though the GPCC has developed a series of gauge-based precipitation analysis datasets with the quality and spatio-temporal resolutions continually improved, accurate estimations of precipitation over the land are still greatly difficult with limited networks of rain gauges. In Asia, great efforts also have been mainly paid on generating gauge-analysis precipitation products at the monthly scale (Chen et al., 2002; Mitchell and Jones 2005; Matsuura and Willmott 2009; Schneider et al. 2008), and limited explorations at the daily scale, e.g., Rajeevan and Bhate (2009) explored daily grid precipitation data over India with data from more than 2,500 rain gauges. Meanwhile, significant differences among those products had been reported by Yatagai et al (2005, 2012). To more accurately monitor and predict the Asian hydro-meteorological environment, the

APHRODITE project (starting in 2006) aimed at developing the state-of-the-art gridded precipitation datasets at the resolutions of 0.25°/daily covering the entire Asia based on the largest numbers of ground observations from multi-sources. Since the release of APHRODITE products (1951-2015, 0.25°/daily, Last update October 5, 2018), APHRODITE daily grid precipitation data sets have been widely used, and it distinguished from other gauge analysis data by considering the different interpolation schemes and climatology characteristics, especially over the mountainous regions with complex terrain, e.g., the Tibetan Plateau (Yatagai et al., 2012).

The aim of this study is to explore the calibration approach at daily scale on the retrospective IMERG data using APHRODITE product, in both TRMM and GPM eras, from 2000 to 2015. Meanwhile, a new calibration approach, Daily Spatio-Temporal Disaggregation Calibration Algorithm (DSTDCA), is proposed and suggested for the GPM in their future algorithms; and a new AIMERG precipitation dataset (0.1°/ half-hourly, 2000-2015, Asia) (Ma et al., 2020a, b) with better quality is to be provided publicly for the Asian applications.

2. Data

2.1 IMERG

To generate the IMERG product, IMERG focused on intercalibrating, merging, and interpolating "all" satellite MW-based precipitation estimates, together with MW-calibrated IR-based precipitation estimates, precipitation gauge analyses, and potentially other precipitation estimators at fine spatio-temporal scales for the both TRMM and GPM eras over the entire globe. Currently, IMERG is at its Version 06 stage (https://pmm.nasa.gov/sites/default/files/document_files/IMERG_ATBD_V06.pdf), based on which IMERG has been retrospect to the TRMM era at the end of September, 2019, and IMERG is now available back to June 2000 (half-hourly/0.1°) (https://pmm.nasa.gov/data-access/downloads/gpm). The "Final run" of IMERG combines the GPCC Monitoring product, the V8 Full Data Analysis for the majority of the time (currently 1998-2016), and the V6 Monitoring Product from 2017 to the then-present. The Monitoring Product is posted about two months after the month of observations from ~7,000-8,000 stations world-wide, which is relative sparse, especially over the Asia (Schneider et al. 2014, 2018).

2.2 APHRODITE

Since the release of the APHRODITE product (0.25°/Daily, 1951-2007), it has been widely used as one of state-of-the-art daily grid precipitation datasets over the Asia, for hydro-climatological related studies (Yatagai et al., 2012; Menegoz et al., 2013; Sunilkumar et al., 2019). APHRODITE has been demonstrated to replicate 'ground truth' observations very well (Duncan and Bigg, 2012) and represents the optimal dataset for analyzing historical precipitation variability and change. Recently, the APHRODITE data has been updated from the former period 1951-2007 to a longer period 1951-2015, in September, 2018, with continuous efforts of quality control (QC) flagging some data (Hamada et al., 2011). The APHRODITE data could be available through the website (http://aphrodite.st.hirosaki-u.ac.jp/download/).

2.3 CMPA

The China Merged Precipitation Analysis (CMPA, 0.1°/hourly, 2008-2015) were generated by using hourly rain gauge data at more than 30, 000 automatic weather stations in China, with the combination of the CMORPH precipitation product, and provided by the Chinese Meteorological Administration (http://data.cma.cn) (Shen et al., 2014). The OI method was adopted to estimate the areal precipitation distribution based on the gauge observations (Yong et al., 2010), but uncertainty still exists in the interpolated precipitation field particularly over West China with relatively sparse gauge networks. For grid boxes with gauges, the observed precipitation values are exactly the gauge observation or the averaged observation when more than one gauge locates in a grid.

2.4 Point-based rain gauge data from meteorological stations

The hourly rain gauge datasets from 57, 835 national ground stations used in this study, in 2015, were collected from the National Meteorological Information Center of CMA (http://data.cma.cn). All the gauge data have undergone strict quality control in three levels, which includes (1) the extreme values' check, (2) internal consistency check, and (3) spatial consistency check (Shen et al., 2010). Most gauges are located over the eastern and southern parts of the Mainland China, and relatively sparse gauge networks are located across the northern and western parts, especially over the Tibetan Plateau. The limited number of gauges could be a source of error in evaluation of satellite precipitation products in such areas (Shen et al., 2014).

2.5 Point-based rain gauge data from hydrological stations

The hourly ground precipitation observations from around 500 hydrological stations (the number of station varied from year to year) used in this study were collected from Hydrology Bureau of Zhejiang Province, southeastern China (http://data.cma.cn/). The quality control follows two steps: (1) the datasets are filtered by threshold value after being collected from rain gauges; (2) the outliers are identified through manual processing. With careful data quality control, the rain gauge datasets have satisfying performances on the accuracy and validity.

There are five datasets used in this study (refer to Table 1 for a summary of the datasets). IMERG and APHRODITE were used for generating the AIMERG data, and the others were used for evaluating and comparing the IMERG and AIMERG at different scales.

Table 1. List of satellite-based, gauge-based, and satellite-gauge combination precipitation products used in this study.

Short name	Full name	Spatial and temporal sampling	Time period	References
IMERG	Integrated Multi-satellitE Retrievals for Global Precipitation Measurement	0.1°/half-hourly	2000-present	Huffman et al. (2019b) https://pmm.nasa.gov/data-access/downloads/gpm (last access: 17 January 2020)
APHRODITE	Asian Precipitation Highly Resolved Observational Data Integration Towards Evaluation of Water Resources	0.25°/daily	1951-2015	Yatagai et al. (2012) http://aphrodite.st.hirosaki-u.ac.jp/download/ (last access: 17 January 2020)
CMPA	China Merged Precipitation Analysis	0.1°/hourly	2008-present	Shen et al. (2014) http://data.cma.cn (last access: 17 January 2020)
	Point-based rain gauge data	hourly	2010-present	Shen et al. (2010) http://data.cma.cn (last access: 17 January 2020)

3. Methodology

3.1 Calibration Procedure of the Daily Spatio-Temporal Disaggregation Calibration Algorithm, DSTDCA

According to previous evaluations on IMERG (Lu et al., 2019; Xu et al., 2019), there are at least two characteristics resulting its significant overestimations: (1) the amplitude of hourly or half-hourly estimated rainfall rates are significantly amplified by IMERG compared with ground observations, which might be caused by the benchmark of GPCC and GPCP SG data for calibrations, and (2) the IMERG algorithm is generally over detecting precipitation events, resulting a large fraction of false alarm but unreal precipitation events. Therefore, this study selects the APHRODITE data as the benchmark for calibrating IMERG at daily scale, based on the proposed approach, DSTDCA, and the main steps of the DSTDCA are shown as follows:

(1) IMERG data (0.1°/half-hourly) are accumulated to IMERG data at the daily scale (0.1°), which are used to generate the spatial disaggregation weights. As the spatial resolution of APHRODITE data is 0.25°, the moving window size of 3 by 3 is selected, and the daily spatial disaggregation weights (0.1°) based on IMERG is obtained by calculating the ratios between the daily rainfall accumulations at the central grid and the average daily rainfall accumulations in the corresponding 3 × 3 window. The daily spatial disaggregation weights consider the relative spatial patterns of the precipitation captured by the IMERG;

(2) Based on the daily precipitation accumulations of IMERG, the half-hourly temporal disaggregation weights (0.1°) are derived by calculating the ratios between the each half-hourly

precipitation estimates and the corresponding daily precipitation estimates. If the daily accumulation estimate is equal to zero, then each half-hourly temporal disaggregation weight is set as zero;

(3) As there is a small fraction of grids in APHRODITE with no data at daily scale, the no data grids in APHRODITE data are firstly filled with the data according to its nearest neighbor with effective value;

(4) Spatial calibrations: the daily calibrated IMERG using APHRODITE data are obtained by multiplying the spatial disaggregation weights based on IMERG (0.1°/daily) from step (1) by daily APHRODITE data (0.25°/ daily) from step (3). In this step, to match the IMERG (0.1°) and APHRODITE (0.25°), the numbers and weights of the APHRODITE grids corresponding to each IMERG pixel are determined, according to the relative spatial locations and coverage relationships between the each pixel of IMERG (0.1°) and the corresponding pixels of APHRODITE (0.25°);

(5) Temporal calibrations: the half-hourly calibrated IMERG are obtained by multiplying the half-hourly temporal disaggregation weights (0.1°/half-hourly) from step (2) by the daily calibrated IMERG from step (4);

(6) By considering the situations that APHRODITE data captured the precipitation while the IMERG did not, the half-hourly calibrated IMERG is further processed by equally disaggregating the value from the daily APHRODITE data at the corresponding grid into 48 half-hourly periods, which are regarded as the half-hourly calibrated IMERG values in the corresponding day;

(7) By considering the situations that IMERG data captured the precipitation while the APHRODITE did not, the 48 half-hourly calibrated IMERG values in corresponding days and locations are all set as zero, to meet the ground truth observations. And this consideration has been already conducted in the fourth step;

After all the above-mentioned procedures, the final calibrated AIMERG (0.1°/ half-hourly) data are obtained by considering both the total precipitation controls and the effective precipitation events measured by the "ground truth" observations by APHRODITE data over the Asia.

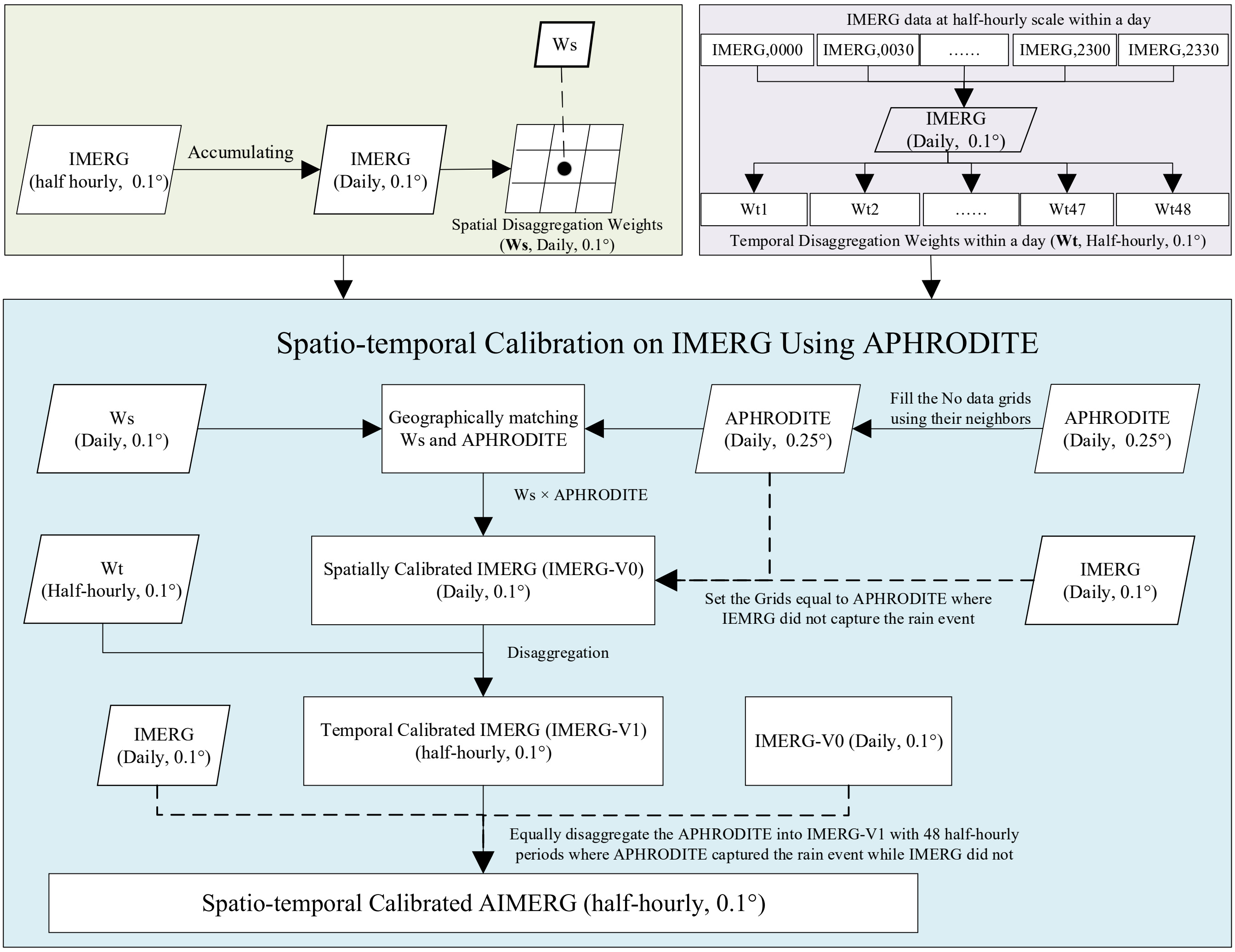

Figure 1. The flowchart of the Daily Spatio-Temporal Disaggregation Calibration Algorithm, DSTDCA, to generate the AIMERG dataset over the Asia, 2000-2015

3.2 Evaluation Metrics

To evaluate the IMERG and its calibrations comprehensively, seven metrics (CC, MAE, BIAS, RMSE, POD, FAR, CSI) were selected (Tang et al., 2016). Generally, CC is used to describe the agreements between satellite estimates and gauge observations; MAE, RMSE, and BIAS are used to indicate the error and bias of satellite estimates compared with gauge observations; and the POD, FAR, and CSI are used to demonstrate the capabilities to correctly capture the precipitation events of satellite precipitation estimates against the ground observations. The detailed information of these evaluation metrics are listed in Table 2.

Table 2 Formulas and perfect values of the evaluation metrics used in this study[a].

Statistic metrics	Equation	Perfect value	Value ranges
Correlation Coefficient (CC)	$\mathrm{CC}=\frac{\frac{1}{N}\sum_{\mathrm{n=1}}^{N}(S_n-\bar{s})(G_n-\bar{G})}{\sigma_S\sigma_G}$	1	[-1, 1]
Mean Error (ME)	$\mathrm{ME}=\sum_{\mathrm{n=1}}^{N}(S_n-G_n)$	0	$(-\infty, +\infty)$
Relative Bias（BIAS)	$\mathrm{BIAS}=\frac{\sum_{\mathrm{n=1}}^{N}(S_n-G_n)}{\sum_{\mathrm{i=1}}^{\mathrm{n}}G_n}\times 100\%$	0	$(-\infty, +\infty)$
Root Mean Square Error (RMSE)	$\mathrm{RMSE}=\sqrt{\frac{1}{N}\sum_{\mathrm{n=1}}^{N}(S_n-G_n)^2}$	0	$[0, +\infty)$
Probability of Detection (POD)	$\mathrm{POD}=\frac{n_{11}}{n_{11}+n_{01}}$	1	[0, 1]
False Alarm Ratio (FAR)	$\mathrm{FAR}=\frac{n_{10}}{n_{11}+n_{10}}$	0	[0, 1]
Critical Success Index (CSI)	$\mathrm{CSI}=\frac{n_{11}}{n_{11}+n_{10}+n_{01}}$	1	[0, 1]

[a]Notation: n is the sample numbers; S_n is satellite precipitation estimate; G_n is gauge-based precipitation; σ_G is the standard deviations of gauge-based precipitation; σ_S is the standard deviations of satellite-based precipitation estimate. n_{11} is the precipitation event detected by both gauge and satellite simultaneously; n_{10} is the precipitation event detected by the satellite but not detected by the gauge; n_{01} is contrary to n_{10}; n_{00} is the precipitation events detected neither by the gauge nor the satellite.

4. Results

4.1 AIMERG Product

Generally, both IMERG and APHRODITE share similar spatial patterns with precipitation volumes decreasing from southeast to northwest in Asia, while compared with APHRODITE data (Fig. 2b), IMERG greatly overestimates the precipitation over Arunachal Pradesh, coastal Indochina and Western Ghats, and the Indonesia (Fig. 2a). Corrected by APHRODITE, the spatial patterns and volumes of AIMERG are much more similar to those of APHRODITE, especially along the Himalayas, coastal Indochina and Western Ghats, and the Indonesia (Fig. 2c). Compared with APHRODITE, AIMERG seems floating up and down in terms of the volumes, for instance, AIMERG is larger and smaller than APHRODITE in eastern Indonesia and northeastern Asia, respectively. Though AIMERG is smaller than IMERG over most regions, there are still some areas where the volumes of AIMERG are larger than those of IMERG, e.g., in western Tibetan Plateau, Middle East, and along the western coast of India (Fig. 2d).

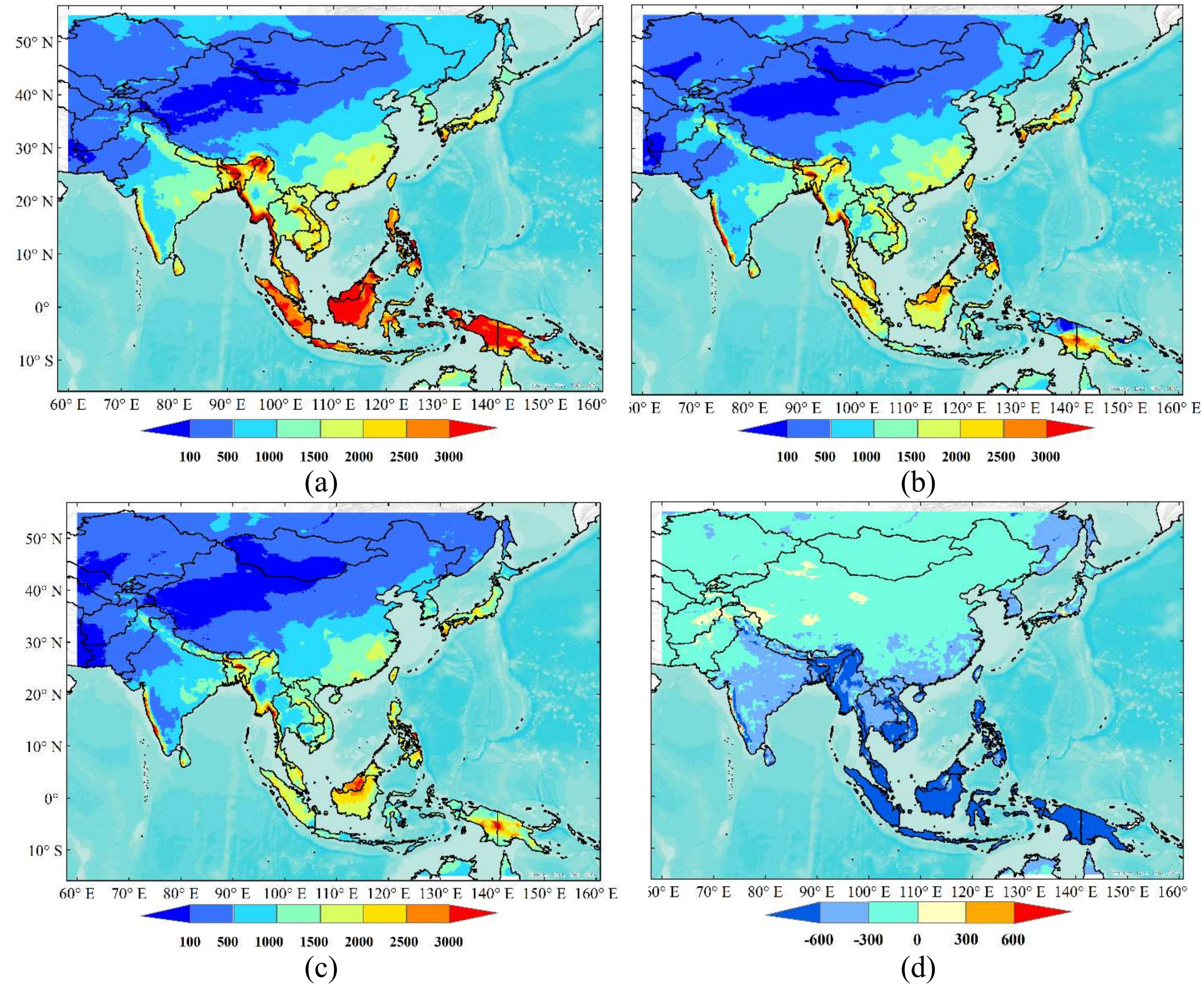

Figure 2. Spatial patterns of Asian mean annual gridded precipitation products of (a) IMERG, 0.1°, (b) APHRODITE, 0.25°, and (c) AIMERG, 0.1°, and (d) AIMERG-IMERG, 0.1°, respectively, during the period of 2001-2015. The background map used in this study was provided by Esri, USGS and NOAA (http://goto.arcgisonline.com/maps/World_Terrain_Base, last access: 17 January 2020).

The temporal patterns of the mean areal precipitation over the Monsoon Asia of the three products demonstrate that the systematic bias of IMERG is significantly reduced in both dry and wet seasons, shown in Fig. 3. IMERG is around 1.5 times larger than APHRODITE at monthly scale. Though much more close to the APHRODITE, AIMERG is still a little smaller than the APHRODITE, which means the calibration algorithm proposed by this study tends to underestimate the precipitation compared with calibration benchmark, APHRODITE. At daily scale, IMERG is generally larger than APHRODITE, while at some special days, APHRODITE is larger than IMERG, which might result the AIMERG may be also larger than IMERG.

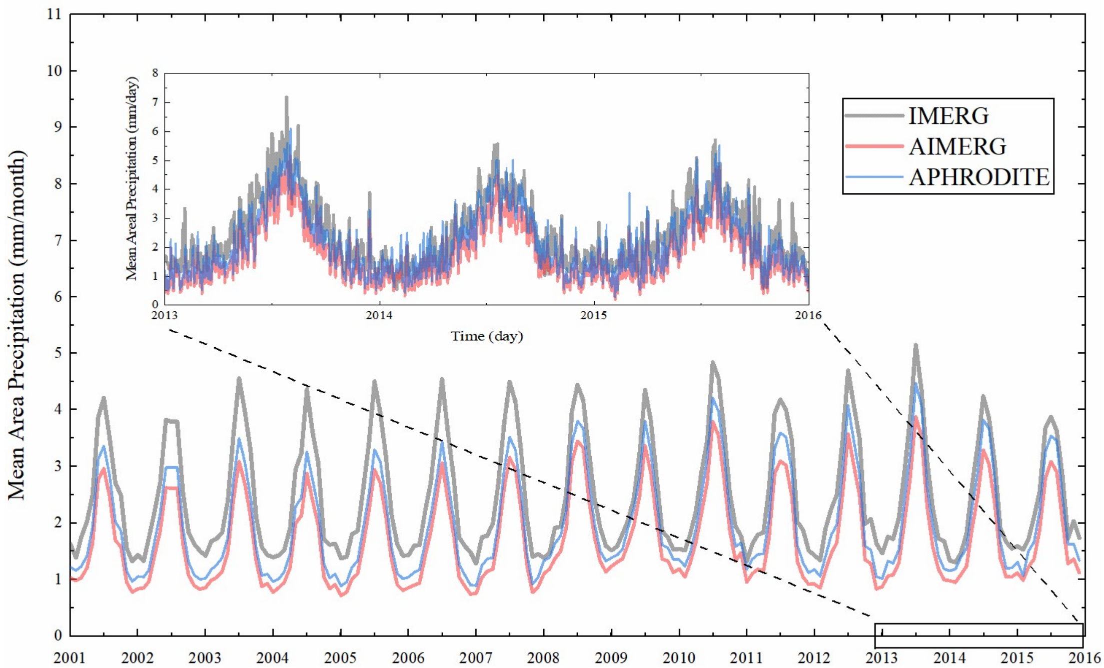

Figure 3. The temporal variations of mean Asian gridded precipitation products of IMERG, APHRODITE, and AIMERG, respectively, during the period of 2001-2015.

4.2 Assessments on IMERG and AIMERG at national and regional scales

The spatial patterns of CMPA demonstrate much more similar to those of AIMERG, especially in the southeastern China where dense rain gauges are located, while both CMPA and IMERG overestimate the precipitation along the Himalayas where the meteorological gauges are sparse and mainly the satellite-based observations are applied (Fig. 4). Obviously, the IMERG significantly overestimates the precipitation in the southeast coast of China, where typhoons always visit (Fig. 4 b). For deciding the sub-regions (Fig. 4 d), we have mainly considered three aspects: the representative climatic zones in China, the local distributions of the gauge stations, and the complexity of the topography. For instances, Sub-Region 1 represents the high latitude plain in the most north-eastern region of China under a cold climate (left top: 115.0° E, 54.0°N; right bottom: 135.0° E, 47.0°N); Sub-Region 2 represents the south-eastern coastal area of China influenced greatly by the Asian Monsoons (left top: 115.0° E, 26.0°N; left bottom: 119.0° E, 24.0°N; right bottom: 124.0° E, 31.0°N; right top: 120.0° E, 34.0°N); Sub-Region 3 represents the most southern region including the island Hainan in the tropical zone (left top: 105.0° E, 24.0°N; right bottom: 115.0° E, 18.0°N); Sub-Region 4 represents the inner area of China covering the Yunnan-Kweichow Plateau and Sichuan Basin, under a humid inland climate (left top: 100.0° E, 33.0°N; right bottom: 107.0° E, 27.0°N); Sub-Region 5 represents the most southern Tibetan Plateau along the

Himalayas with complex terrains and high elevations above ~ 4000.0 meters (left top: 80.0° E, 33.0°N; right bottom: 95.0° E, 27.0°N); Sub-Region 6 represents the central Asia with complex terrains covering the entire Tianshan Mountains in China under an arid inland climate (left top: 80.0° E, 45.0°N; right bottom: 92.0° E, 40.0°N).

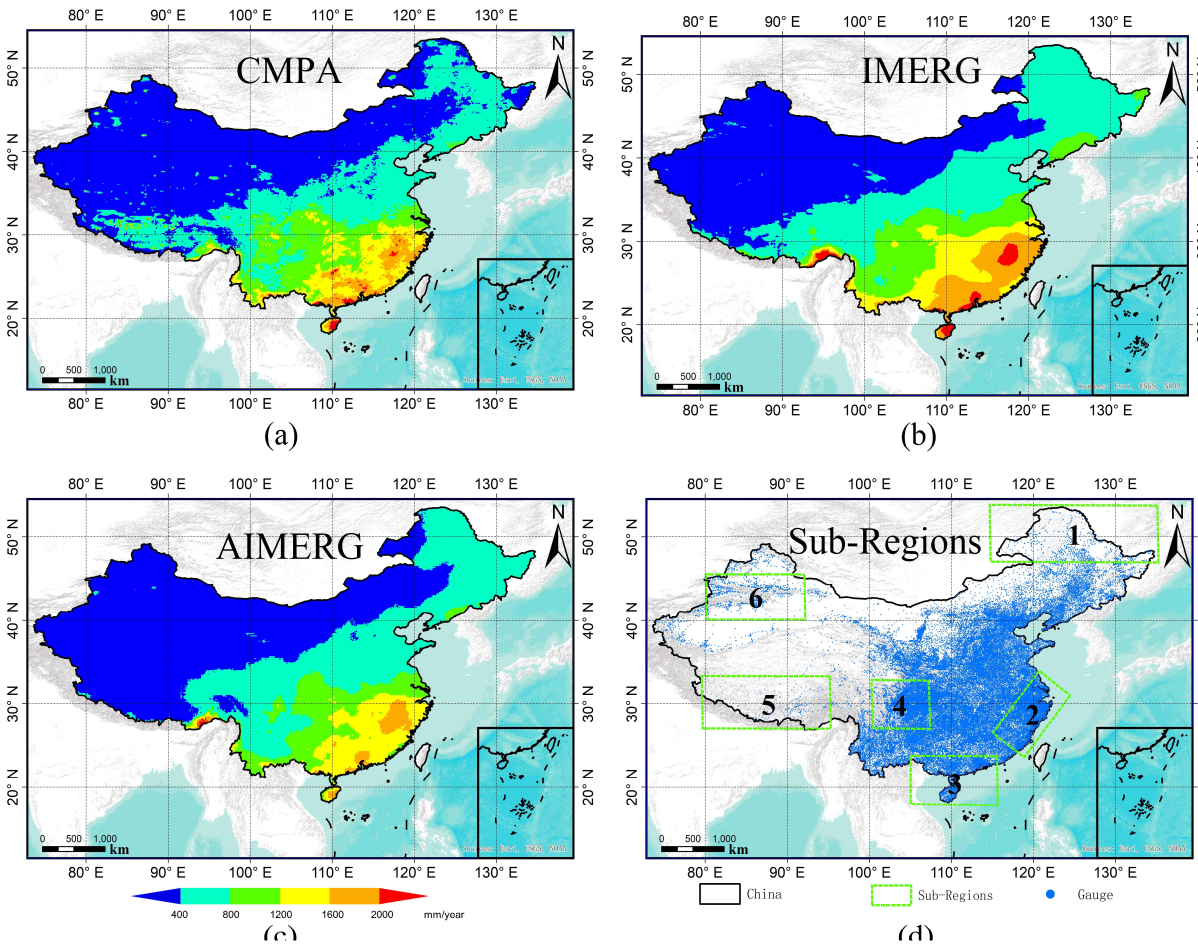

Figure 4 Spatial patterns of (a) CMPA, (b) IMERG, and (c) AIMERG over China Mainland From 2008~2015, and (d) the spatial distributions of the ~ 50, 000 automatic meteorological stations in China Mainland. The accurate boundary information of the Sub-Regions: Sub-Region 1 (left top: 115.0° E, 54.0°N; right bottom: 135.0° E, 47.0°N); Sub-Region 2 (left top: 115.0° E, 26.0°N; left bottom: 119.0° E, 24.0°N; right bottom: 124.0° E, 31.0°N; right top: 120.0° E, 34.0°N); Sub-Region 3 (left top: 105.0° E, 24.0°N; right bottom: 115.0° E, 18.0°N); Sub-Region 4 (left top: 100.0° E, 33.0°N; right bottom: 107.0° E, 27.0°N); Sub-Region 5 (left top: 80.0° E, 33.0°N; right bottom: 95.0° E, 27.0°N); Sub-Region 6 (left top: 80.0° E, 45.0°N; right bottom: 92.0° E, 40.0°N). The background map used in this study was provided by Esri, USGS and NOAA (http://goto.arcgisonline.com/maps/World_Terrain_Base, last access: 17 January 2020).

The magnitudes of IMERG, AIMERG, and CMPA are compared at national and regional scale over the China Mainland from 2008 to 2015 (Fig. 5). Generally speaking, CMPA and AIMERG are almost same, and are significantly smaller than IMERG at both annual and monthly scales, additionally, CMPA is still a little larger than AIMERG over the China Mainland, which could be possibly resulted from the use of satellite observations in the CMPA and IMERG (Fig. 6a). The overall situations of the three product in sub-region 1 and 2 are similar with those over the China Mainland (Fig. 6 b-c), while both CMPA and IMERG are both significantly larger than AIMERG (Fig. 6 d-f). In sub-region 6, the Tianshan

Mountains, CMPA is almost even larger than IMERG, which indicates that large uncertainties should be focused on sub-region 6 (Fig. 6 g).

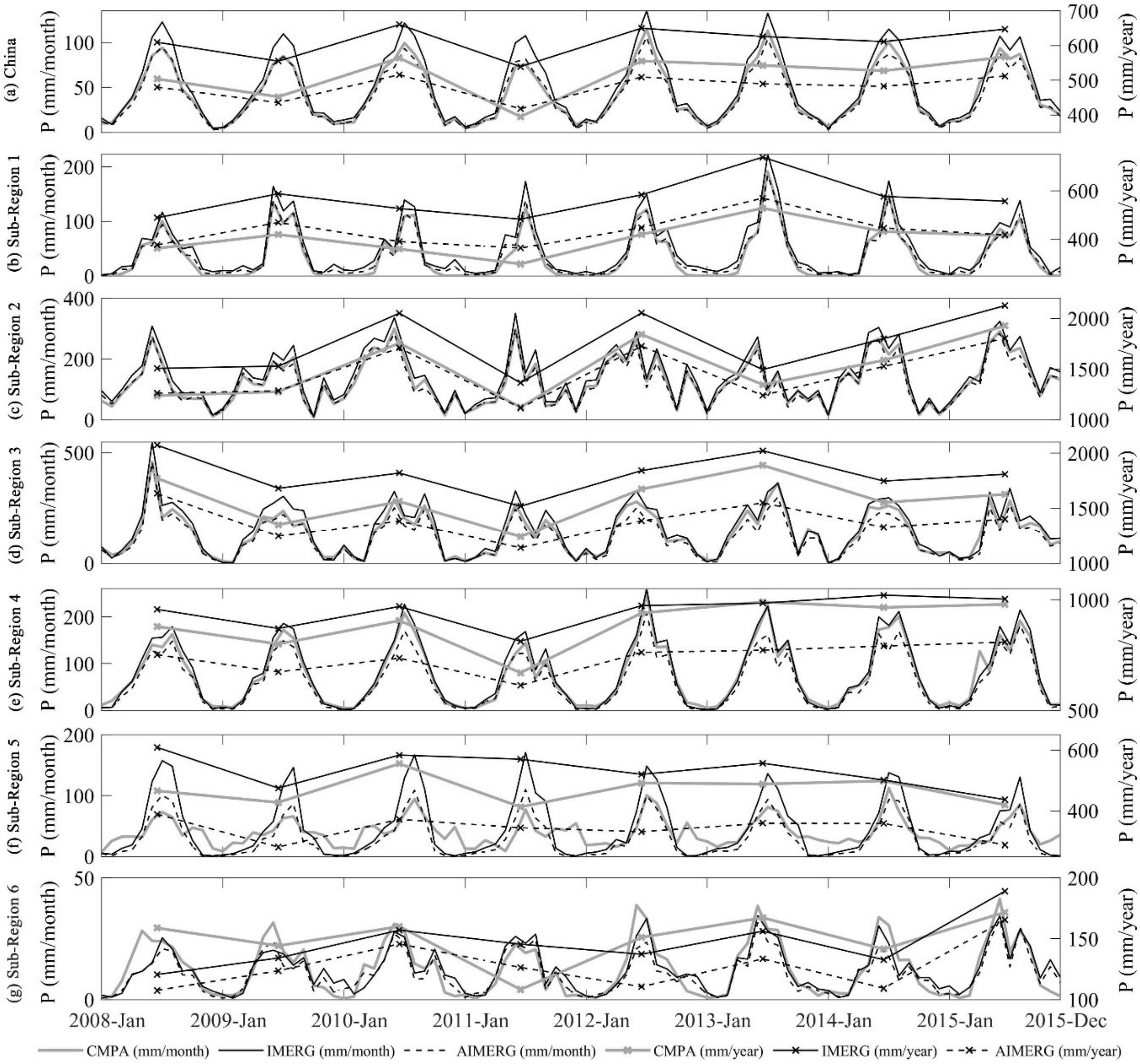

Figure 5 The temporal patterns of mean areal precipitation of the IMERG, CMPA, and AIMERG, over China Mainland and sub-regions from 2008 to 2015, at monthly and annual scales.

As this study aims to propose a new algorithm for calibrating the IMERG product at the daily scale, the daily spatial patterns of IMERG, CMPA, and AIMERG were explored, which generally agree with those of IMERG, CMPA, and AIMERG at monthly scale (Fig. 6). In mountainous region, along the Himalayas, with relatively small precipitation, CPMA is greatly larger and smaller than the other two products (both IMERG and AIMERG) in dry seasons and wet seasons respectively (Fig. 6 f). One phenomenon should be noted that the CPMA seems abnormal along the Himalayas, which might be resulted by the limited ground observations used in CMPA, shown in Fig 4d, while APHRODITE data integrate large numbers of ground observations from the neighbor countries, such as India, Nepal, Bhutan, providing valuable information for retrieving high quality precipitation product around the Tibetan Plateau (Yatagai, 2012). Calibrated by APHRODITE at daily scale, AIMERG is significantly smaller than IMERG and CMPA at both annual and monthly scale, while there are also some situations that AIMERG is larger than IMERG and CMPA at daily scale, for example in sub-region 6, over the Tianshan mountains.

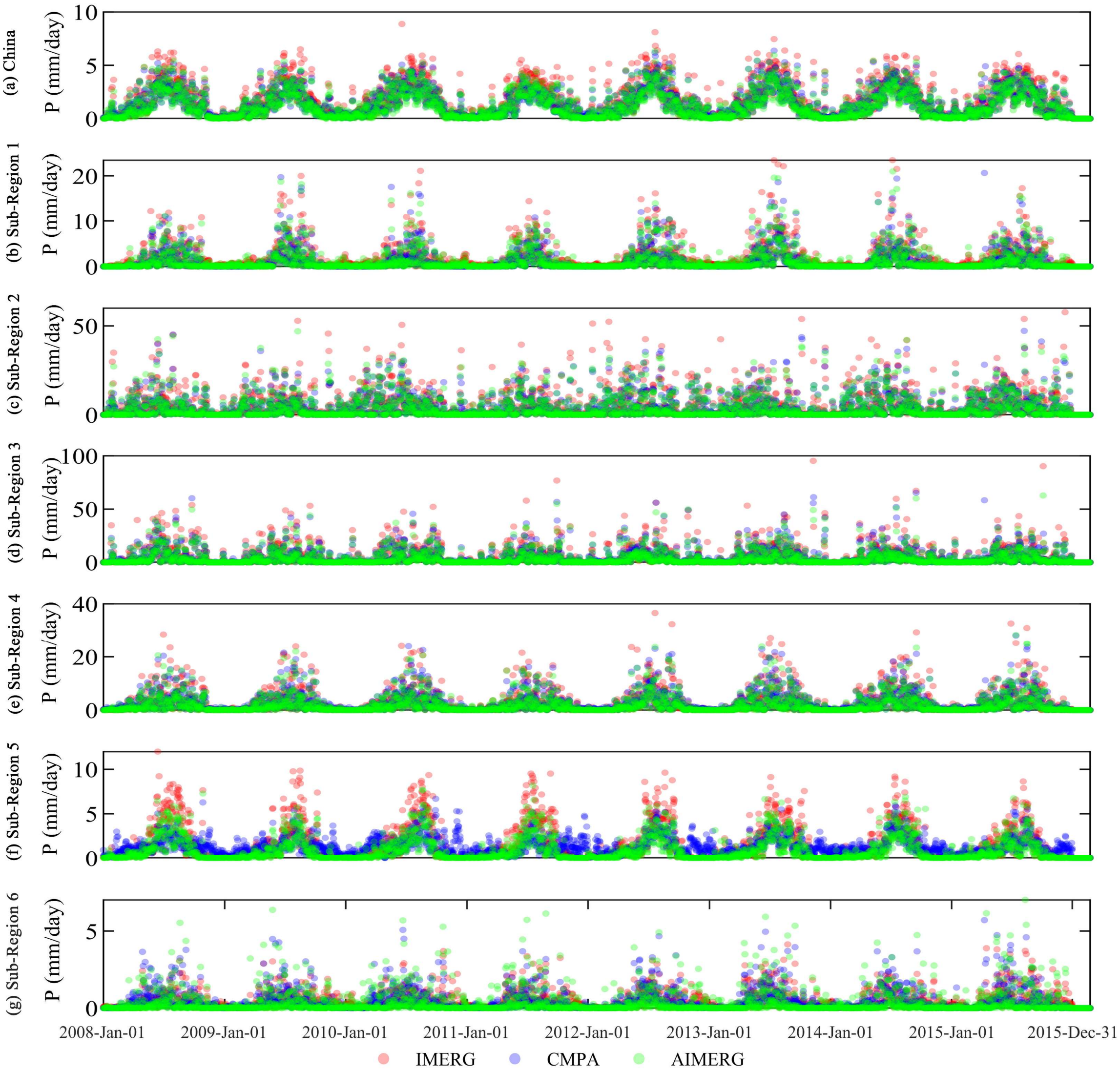

Figure 6. The temporal patterns of mean areal precipitation of the IMERG, CMPA, and AIMERG, over China Mainland and sub-regions from 2008 to 2015, at daily scale.

Hourly ground observation data from more than 50, 000 meteorological stations were used to assess the quality of the IMERG and its calibrations, AIMERG, over the six sub-regions, in 2015 (Fig. 7). The temporal patterns and volumes of mean areal precipitation by AIMERG and ground observations are almost same, while IMERG is generally larger than AIMERG and ground observations. Meanwhile, the IMERG still has the problems in overestimating and underestimating the precipitation in dry seasons (relatively large precipitation occurring) and wet seasons (relatively small precipitation happening), respectively, for example in sub-region 6, over the Tianshan Mountains. In terms of quantitative indices (Standard deviation, RMSD, and CC), AIMERG generally outperforms the IMERG against the ground observations, especially in sub-region 5, along the Himalayas, which indicates that the ground information from the neighbor countries integrated into the APHRODITE data greatly benefits the calibration results, AIMERG.

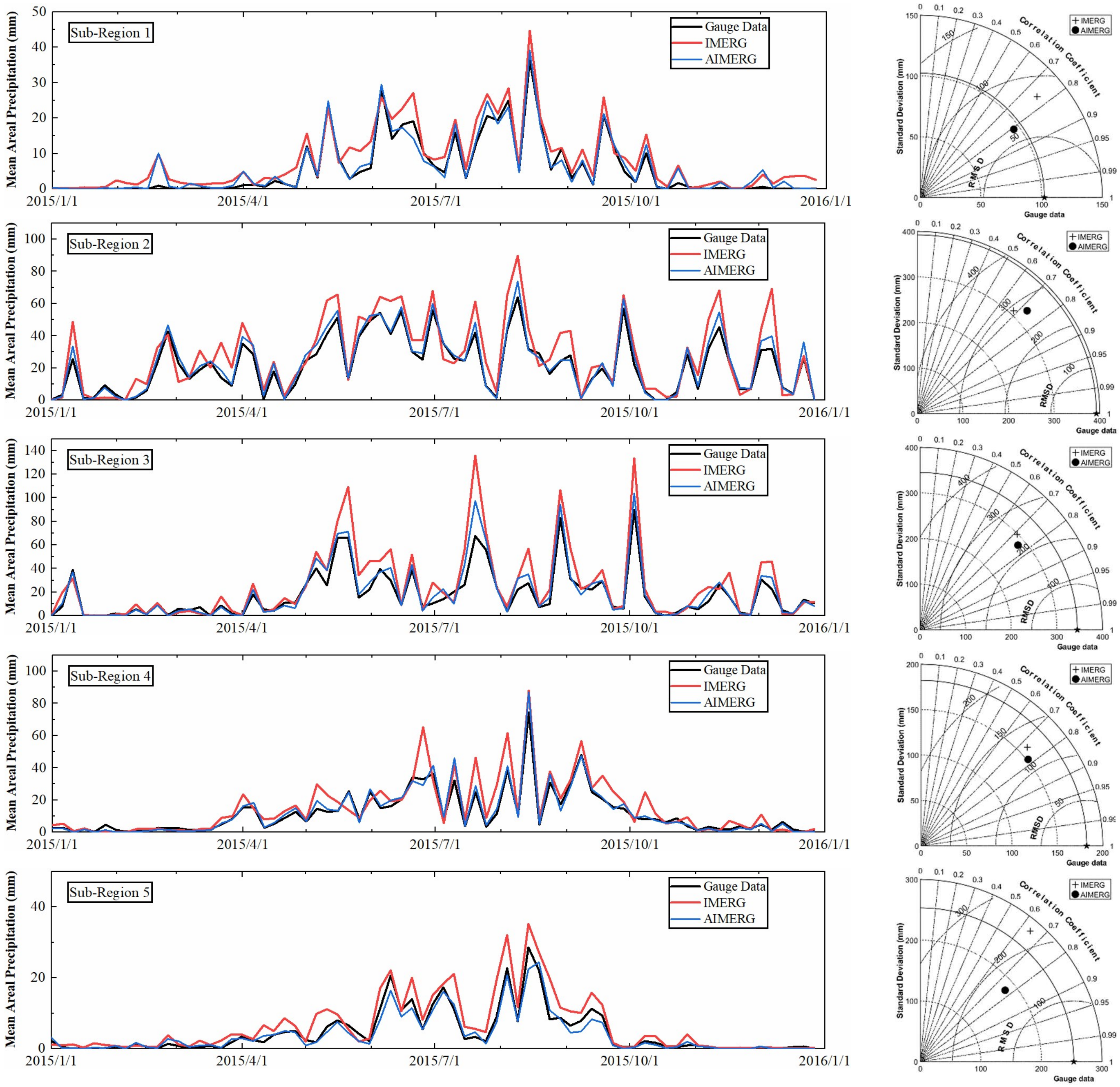
Sub-Region 1
Sub-Region 2
Sub-Region 3
Sub-Region 4
Sub-Region 5
Gauge Data
IMERG
AIMERG
Mean Areal Precipitation (mm)
2015/1/1
2015/4/1
2015/7/1
2015/10/1
2016/1/1
Correlation Coefficient
Standard Deviation (mm)
Gauge data
RMSD

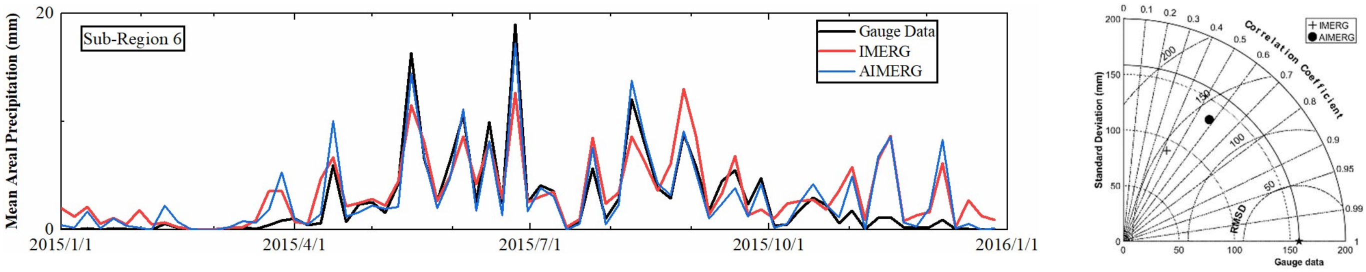

Figure 7. The temporal patterns and the volumes of IMERG, ground observations, and AIMERG, in six sub-regions at daily scale; and the Taylor diagrams of performances on IMERG and AIMERG against ground observations in terms of centered root-mean-square difference, correlation coefficient and standard deviation in the six sub-regions at hourly scale, in 2015.

Figure 8 illustrates the numerical distributions of contingency statistics for IMERG and AIMERG, at hourly scale, in six sub-regions, 2015. Generally, the POD values of AIMERG are larger than those of IMERG (Fig. 8a), and FAR values of AIMERG are overall smaller than those of IMERG in each sub-regions (Fig. 8b), which results the better performances of the comprehensive index, CSI, combining both the characteristics of POD and FAR, in each sub-regions (Fig. 8c). Additionally, both the IMERG and AIMERG perform best in sub-region 2, and worst in sub-region 3.

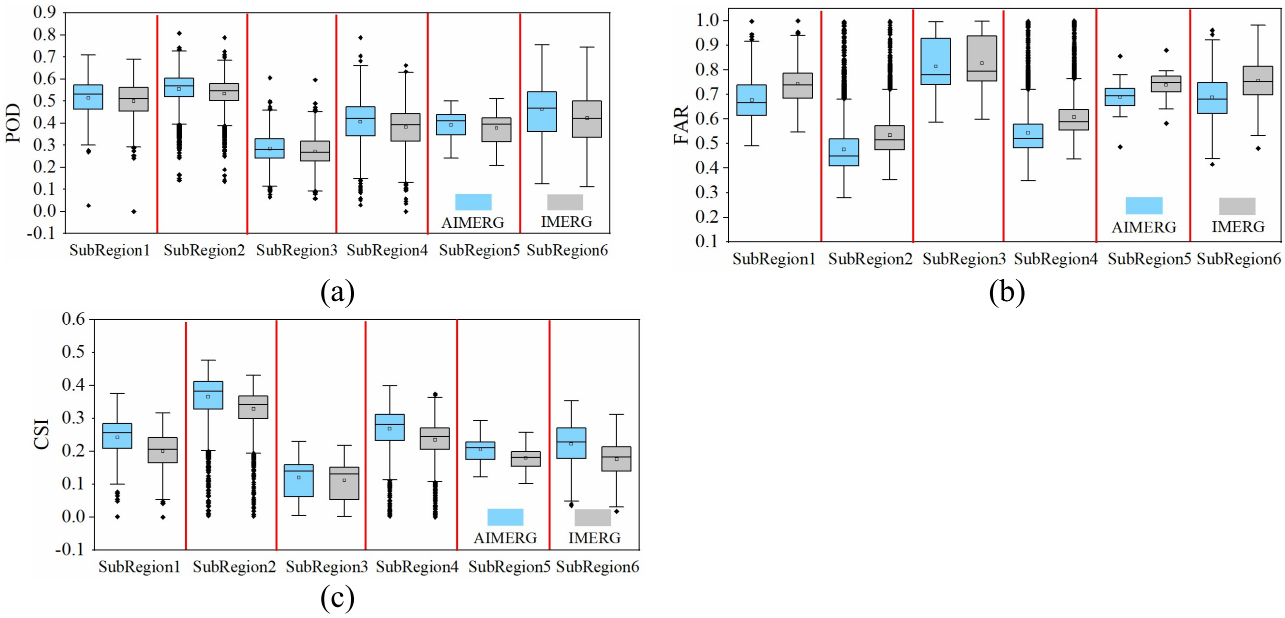

Figure 8. The boxplots demonstrate diagnose of IMERG and AIMERG against the ground observations from the meteorological stations, at hourly scale, in six sub-regions, 2015.

To assess the quality of the IMERG and AIMERG, entirely independent precipitation data from around 500 hydrological stations, at hourly scale, from 2010 to 2015, were applied, which are relatively even distributed in Zhejiang province (Fig. 9a). The POD values of AIMERG (~ 0.9) are general larger than those of IMERG (~ 0.8), while the FAR values of AIMERG (~ 0.3) are significantly smaller than those of IMERG (~ 0.4), which results in the overall capabilities of AIMERG to capture the precipitation events are improved more than 10%, compared with IMERG, in terms of the CSI. The relative smaller POD values and larger FAR values of IMERG in the Zhejiang province, southeastern coast of China, might be one of the potential drawbacks in accurately estimating the precipitation both qualitatively and quantitatively.

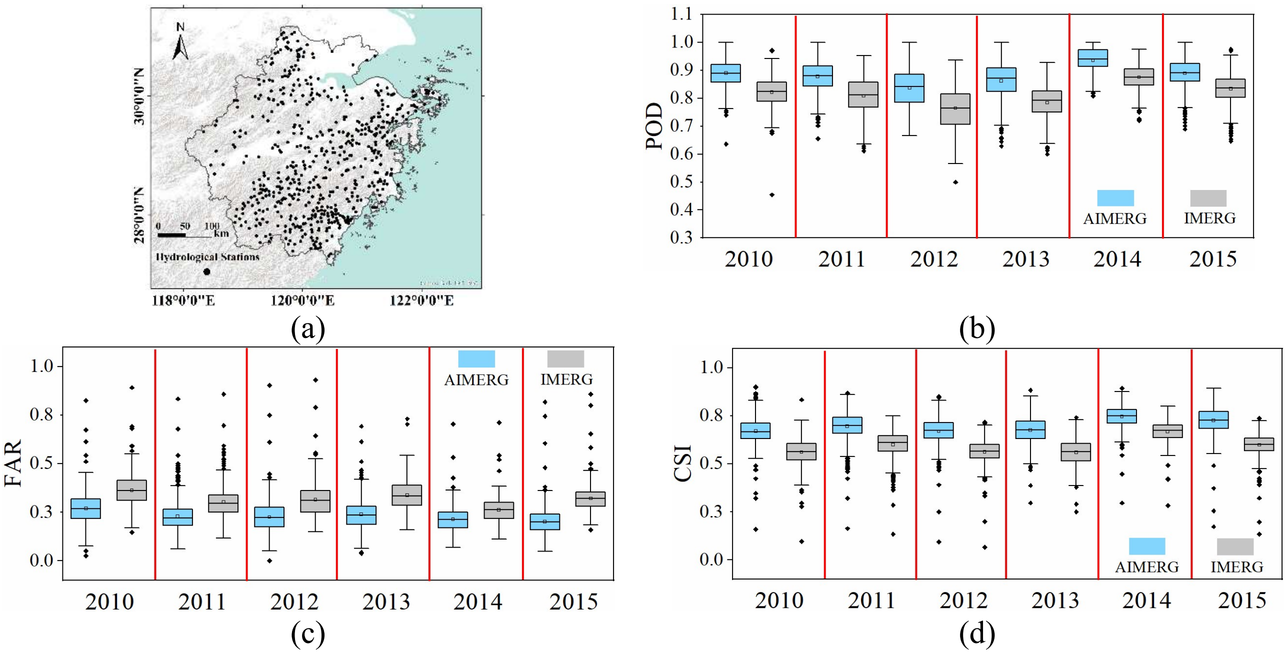

Figure 9. The boxplots demonstrate diagnose of IMERG and AIMERG against the ground observations from hydrological stations, respectively, at hourly scale, in Zhejiang province, 2010-2015. The background map used in this study was provided by Esri, USGS and NOAA (http://goto.arcgisonline.com/maps/World_Terrain_Base, last access: 17 January 2020).

From the temporal patterns of mean areal precipitation of IMERG, AIMERG, and ground observations from hydrological stations, in Zhejiang province, 2010-2015 (Fig. 10), IMERG is general larger than both AIMERG and ground observations. For instance, the IMERG significantly overestimates the precipitation with up to ten times than that of AIMERG and ground observations, such as in the typical periods, 0 a.m., June, 11 – 0 a.m., June, 14, 2015, and 0 a.m., Aug, 29 – 0 a.m., Sep, 1, 2015. Additionally, both the temporal patterns and the magnitudes of AIMERG are almost same with those of ground observations, compared with those of IMERG. Meanwhile, in some pentads with the heavy rain events, both AIMERG and ground observations are larger than IMERG.

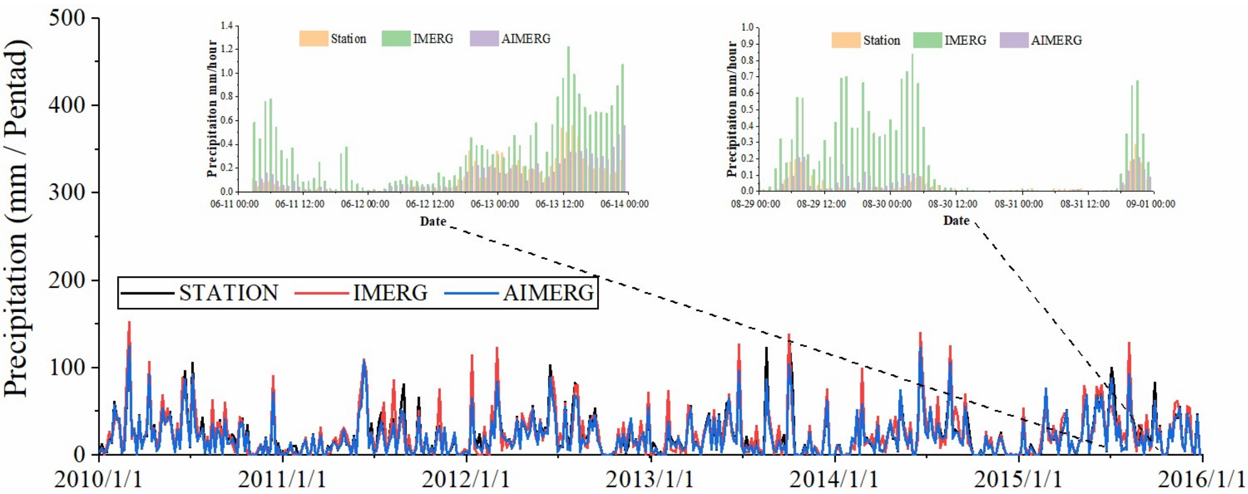

Figure 10. The temporal patterns of mean areal precipitation of IMERG, AIMERG, and the ground observations from the independent hydrological stations, at daily/hourly scale, in Zhejiang province, 2010-2015.

One of the primary aims of the satellite-based precipitation estimates is to provide the high quality precipitation information at hourly scale in the heavy rainfall events. Therefore, one typhoon event, Chan-hom, is selected as an example for assessing the quality of the IMERG and AIMER in Zhejiang Province, where is always threatened by the typhoons, shown in Fig. 11. Though the spatial patterns of IMERG and AIMERG are both similar to those of ground observations, IMERG still underestimates the precipitation, compared with AIMERG (Fig. 11 a-c). From the statistics, not only the systematic bias of IMERG (around -50%) is significantly improved, with bias of AIMERG around -10%, but also the random errors of IMERG (RMSE ~ 2.7 mm/hour, MAE ~ 1.5 mm/hour) are also reduced, compared with AIMERG (RMSE ~ 2.5 mm/hour, MAE ~ 1.4 mm/hour), which meant the calibrations using APHRODITE on IMERG improved the abilities of original IMERG product to more accurately estimate the quantitative precipitation volumes, especially in heavy rainfall events (Fig. 11 c-d).

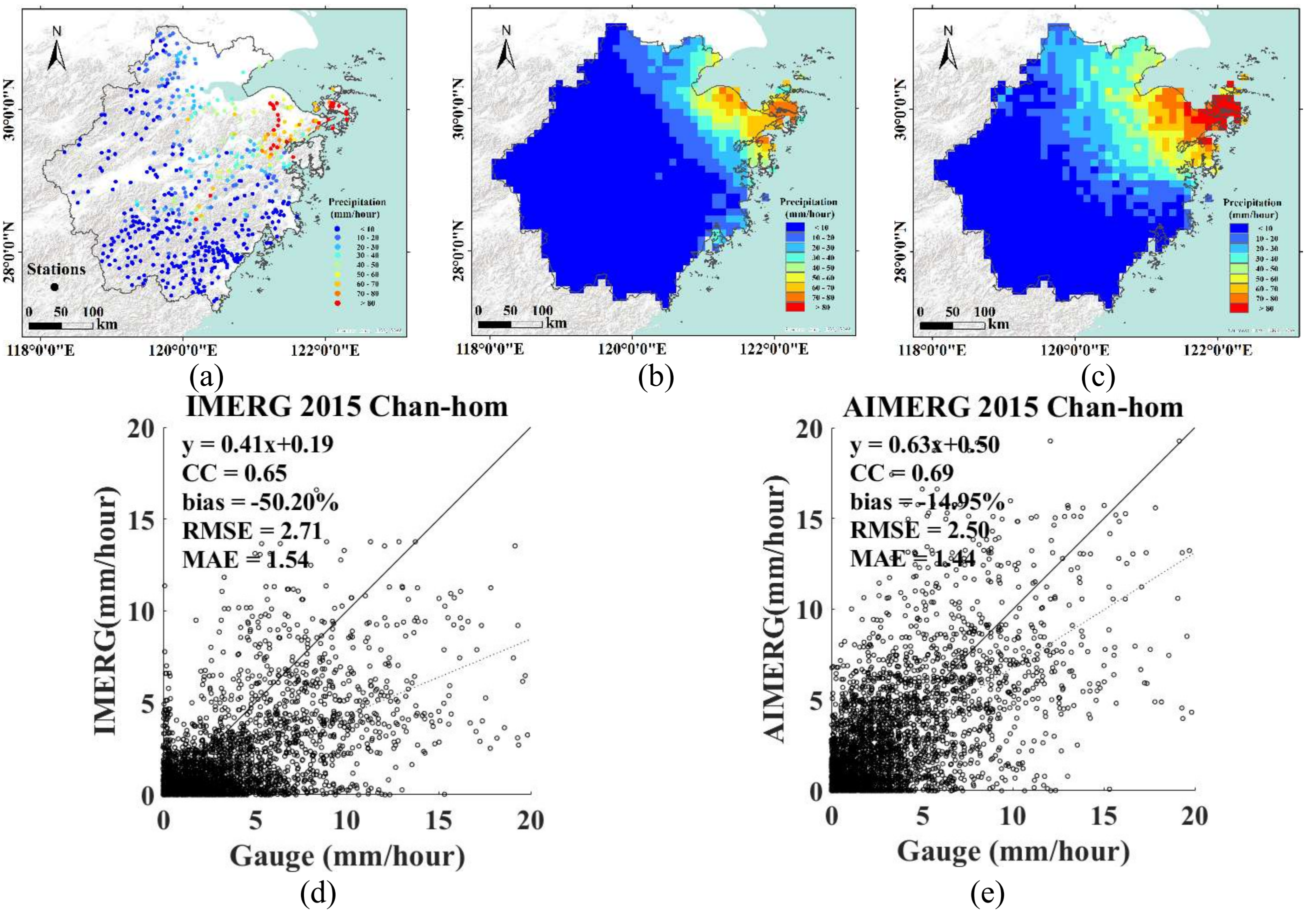

Figure 11. The typhoon, Chan-hom, is selected as an example for assessing the quality of the IMERG and AIMER, occurred in the typical period 0 a.m., – 11 a.m., July, 11, 2015, in Zhejiang Province. The background map used in this study was provided by Esri, USGS and NOAA (http://goto.arcgisonline.com/maps/World_Terrain_Base, last access: 17 January 2020).

5. Discussions

5.1. The potential drawbacks in processing the IMERG product

From the document of "Algorithm Theoretical Basis Document (ATBD) Version 06" for generating the final IMERG product (Huffman et al., 2019a), we find that there are mainly two steps in the process: the first step is to derive the multi-satellite only precipitation inversion estimates, and the second step is to calibrate the satellite-based only precipitation estimates using the interpolated precipitation product based on ground observations, e.g., GPCC (1.0°/monthly). As lacking mature calibration algorithm for calibrating the multi-satellite-only precipitation estimates at daily scale, the current IMERG-Final product are only calibrated using the GPCC at monthly scale. The two aims of this study are to (1) provide a spatio-temporal calibration algorithm (DSTDCA) for anchoring the satellite-based precipitation estimates at daily scale, and (2) a new precipitation product with finer quality, namely AIMERG (half-hourly, 0.1°×0.1°, 2000-2015, Asia) (Ma et al., 2020a, b), for Asian researcher. For anchoring the IMERG final product, we introduce the APHRODITE data (daily, 0.25°×0.25°, 2000-2015, Asia), which were interpolated based on ground observations from the large numbers of rain gauges. Though the general spatial patterns of monthly mean precipitation estimates from both APHRODITE and GPCC, from 1951 to 2015, are similar, the volumes of them demonstrate significant differences, especially along the Himalayas, coastal Indochina and Western Ghats, and the Indonesia (Fig. 12 a-b). To much more clearly demonstrate the relative values of GPCC and APHRODITE, the spatial patterns of the ratio of monthly mean values of APHRODITE to those of GPCC are illustrated in Fig. 12 c, from which we find that GPCC significantly overestimates the precipitation in the tropical rain range along the Indonesia, and along the southern Himalayas with complex terrain, while it significantly underestimates the precipitation in the north western Tibetan Plateau and Middle East, compared with the ground “truth” product, APHRODITE. Illustrated by Fig. 12, the GPCC plays vital roles for the final IMERG product, and the introduction of APHRODITE on calibrating the IMERG would be greatly benefiting the quality of the AIMERG.

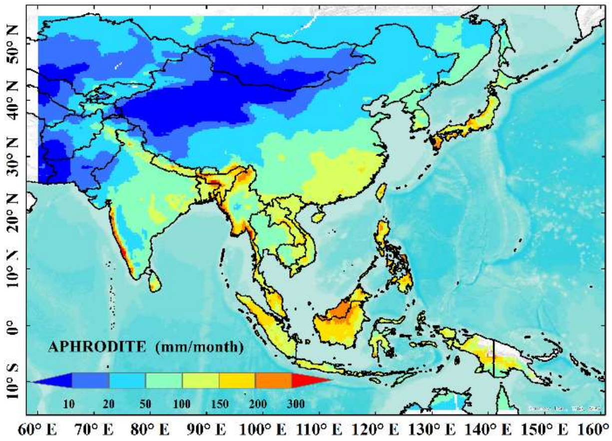

(a)

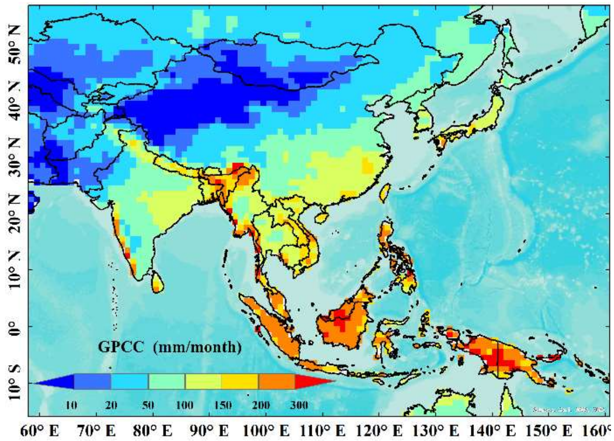

(b)

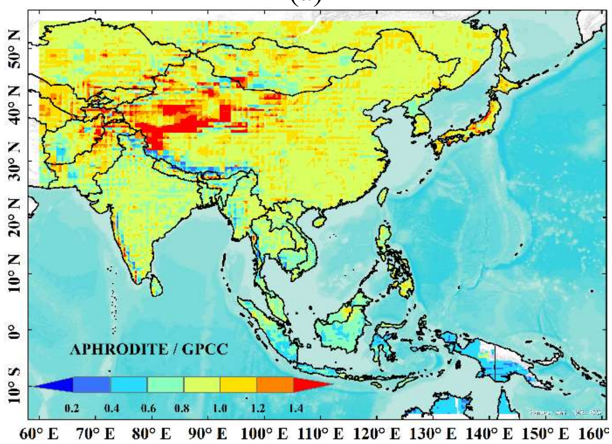

(c)

Figure 12. The spatial patterns of the monthly mean precipitation of (a) APHRODITE and (b) GPCC, and (c) Ratios between monthly mean values of APHRODITE and GPCC, over the Asia in the period from 1951 to 2015. The background map used in this study was provided by Esri, USGS and NOAA (http://goto.arcgisonline.com/maps/World_Terrain_Base, last access: 17 January 2020).

There are mainly two kinds of errors in the multi-satellite-only precipitation product, including systematic bias and random errors (Shen et al., 2014). As seen in the above-mentioned results, the random errors of the AIMERG are alleviated by using the APHRODITE data compared with IMERG (e.g., Fig. 4-11). In terms of the systematic errors, we compared the monthly Asian mean precipitation estimates of both APHRODITE and GPCC, from 1951 to 2015 (Fig. 13). The monthly Asian mean precipitation of APHRODITE varies between ~ 25 mm/month and ~ 100 mm/month, while those of GPCC ranges from ~ 50 mm/month and ~ 150 mm/month, which results the ratios of APHRODITE to GPCC fluctuate significantly from ~ 0.2 to ~ 0.9, with average value ~ 0.7, which means that the GPCC at least overestimates the precipitation more than ~ 30%, compared with the APHRODITE. Therefore, the introduction of APHRODITE data would greatly reduce the systematic errors of the IMERG final product, over the Asia.

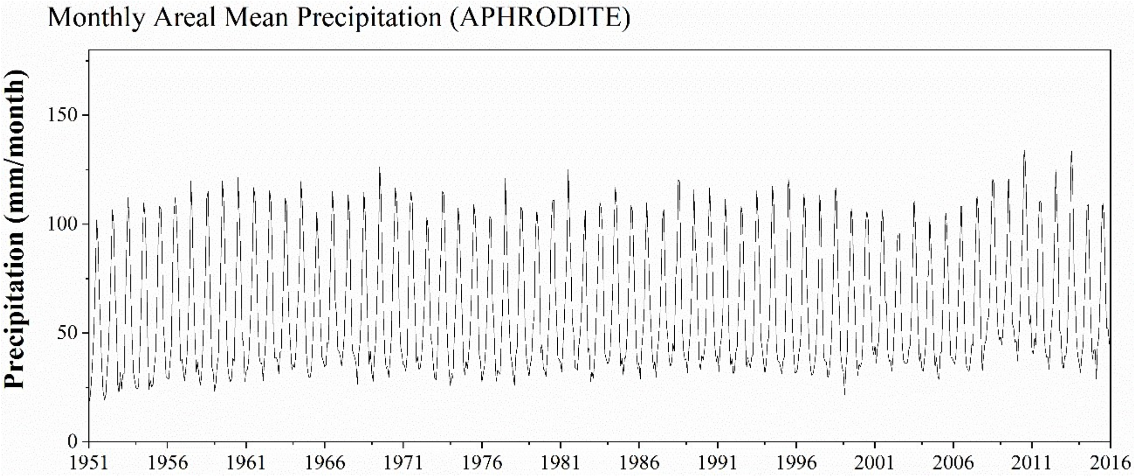
Monthly Areal Mean Precipitation (APHRODITE)
Precipitation (mm/month)
0
50
100
150
1951
1956
1961
1966
1971
1976
1981
1986
1991
1996
2001
2006
2011
2016
(a)

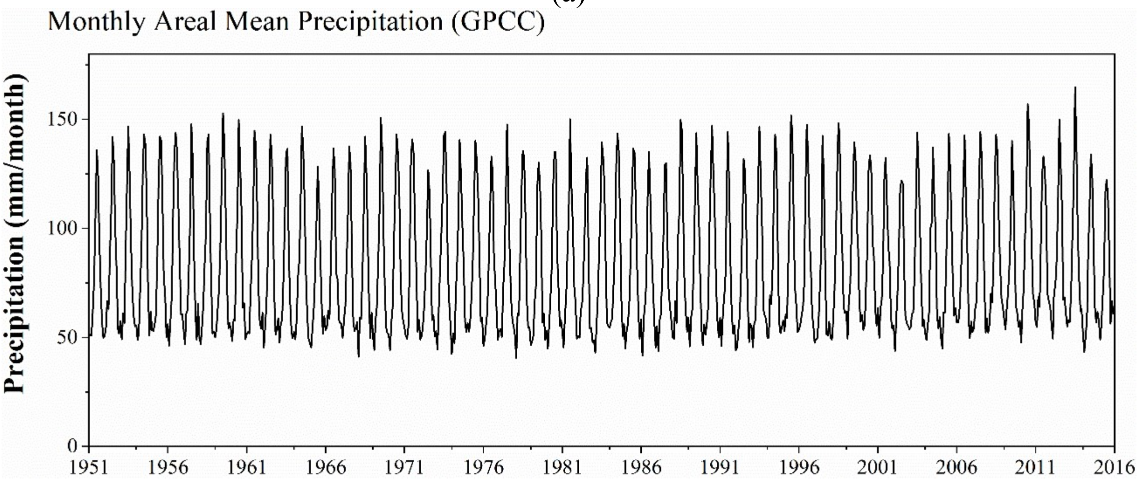
Monthly Areal Mean Precipitation (GPCC)
Precipitation (mm/month)
0
50
100
150
1951
1956
1961
1966
1971
1976
1981
1986
1991
1996
2001
2006
2011
2016
(b)

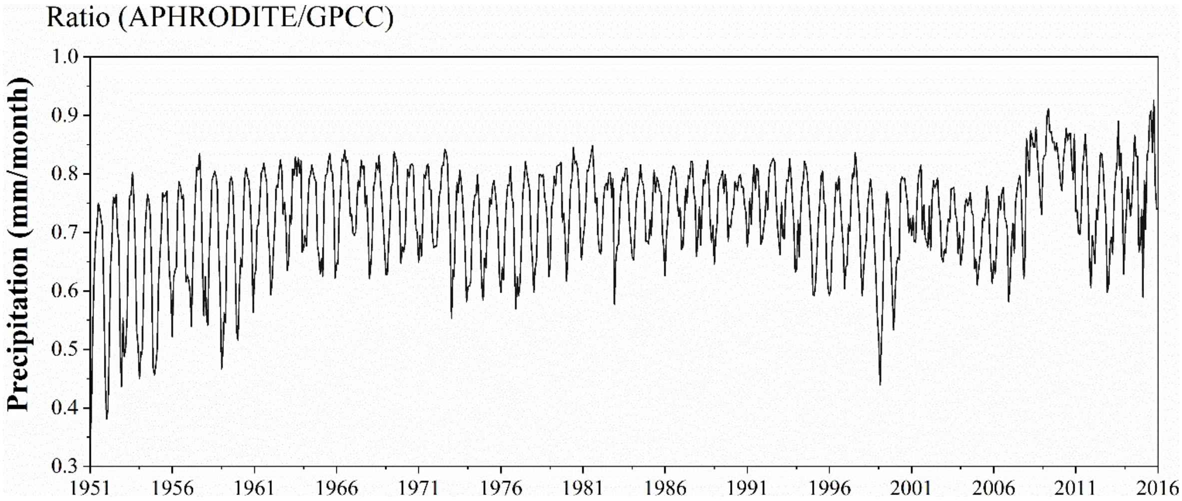

(c)

Figure 13. The temporal patterns of monthly areal mean precipitation of (a) APHRODITE, (b) GPCC, and (c) APHRODITE/GPCC, 1951-2015.

5.2. The controls on the range of the spatial weights based on IMERG

As demonstrated in the document of the "ATBD", gauge information is introduced into the original multi-satellite-only half-hourly data to generate the final IMERG product. Firstly, the ratio between the monthly accumulation of half-hourly multi-satellite-only field and the monthly satellite-gauge field is calculated, then each half-hourly field of multi-satellite-only precipitation estimates in the corresponding month is multiplied by the ratio field to generate the half-hourly calibrated IMERG. After various experiments, the ratio values between the monthly satellite-gauge and the monthly accumulation of half-hourly multi-satellite-only fields is limited to the range [0.2, 3] (Huffman et al., 2019a). The cap of 3 is decided due to the value of 2 (used in TRMM V6) was too restrictive. Additionally, the cap of 3 was finally applied because it performed better in matching the two accumulations than that of other larger values, for instance, the cap of 4 resulted in introducing unrealistic shifts to histogram of half-hourly precipitation rates for the month. Additionally, early in TRMM the lower bound of 0.5 was applied, which suggested a smaller value of the lower bound allows matching between the two accumulations without creating the egregious high snapshot values when the upper bound was expanded too far.

Inspired by the range of the ratio values between the monthly satellite-gauge and the monthly accumulation of half-hourly multi-satellite-only fields in generating IMERG, we consider the range [0, 1.5] of the daily spatial disaggregation weights in this study is reasonable after careful checking the distributions of spatial disaggregation weights. The lower bound of 0 was selected based on the consideration if the IMERG did not capture the daily precipitation event, then the spatial disaggregation weight is still equal to zero, which agrees as most as possible to the original IMERG. While there are at least two reasons for setting the upper bound of the spatial disaggregation weights as 1.5: (1) most numerical values of spatial disaggregation weights are in the range [0, 1.5], and (2) there are obvious anomalies in the final calibrated AIMERG, especially along the coastal regions and edges of the specific precipitation event coverages, where the values of the spatial disaggregation weights are larger than 1.5. Though the range [0, 1.5] of spatial disaggregation weights was applied to obtain the final AIMERG in this study, we also consider that this is still an open-ended question.

5.3. The advantages of APHRODITE data in anchoring the multi-satellite-only precipitation product

It has been a great challenge to obtain precipitation estimates over the Tibetan Plateau and its surroundings, as there are very limited ground observations in this region, especially in its western parts (Ma et al., 2017). Incorporating a uniform precipitation gauge analysis is important and critical for controlling the bias that typifies the satellite precipitation estimates, e.g., using GPCC for TMPA and IMERG (Huffman et al., 2019a). Those projects (e.g., GPCC, TRMM, GPM) demonstrate that even monthly gauge analyses contribute significant improvements on the satellite-only precipitation estimates, at least for some regions in some seasons. Primarily explorations at CPC suggested substantial improvements in the bias corrections using daily gauge analysis, especially for regions, where there is a dense network of gauges (Mega et al., 2014). Foreseeably, GPM would try their best to calibrate the GPM multi-satellite only precipitation estimates at finer spatio-temporal scales (e.g., 0.25°/daily) worldwide.

Currently, GPCC has been adopted to calibrate the TRMM TMPA and GPM IMERG at monthly scale. The Deutscher Wetterdienst (DWD) Global Precipitation Climatology Centre (GPCC) was established in 1989 to provide high-quality precipitation analyses over land based on conventional precipitation gauges from ~7,000-8,000 stations world-wide (Schneider et al. 2014, 2018). And two GPCC products were applied in the IMERG, the V8 Full Data Analysis for the majority of the time (currently 1998-2016), and the V6 Monitoring Product from 2017 to the then-present. Compared with

GPCC, APHRODITE has inherently advantages with significantly larger numbers of ground observations and finer spatio-temporal resolutions, over the Asia. APHRODITE projects aimed at collecting as most gauge information as possible from the Asian countries. There are mainly three kinds of gauge information sources used in APHRODITE analysis, the GTS-based data, data precompiled by other projects or organizations, and APHRODITE's own collection. More detailed information on the APHRODITE' data sources could be found at the website (http://www.chikyu.ac.jp/precip/) and the research of Yatagai (2012). Compared with the GPCC with the limited ground observations in and around the Tibetan Plateau in China, the neighboring countries provide plenty of ground observations in the APHRODITE data, in mountainous regions, and semi-arid and arid regions. Additionally, the spatio-temporal resolutions of APHRODITE (0.25°/daily) are finer than those of GPCC (1.0°/monthly). Therefore, APHRODITE has significant advantages in calibrating the IMERG data at daily scale.

5.4. Quantitatively and horizontally comparisons with other high resolution precipitation product

Recently, Tang et al (2020) has conducted a comprehensive comparison of GPM IMERG with other nine state-of-the-art high resolution precipitation products, six satellite-based precipitation products (TRMM 3B42, 0.25°/3 hour; CMORPH, 0.25°/3 hour; PERSIANN-CDR, 0.25°/1 day; GSMaP 0.1°/1 hour; CHIRPS, 0.05°/1 day; SM2RAIN, 0.25°/1 day) and three reanalysis datasets (ERA5, ~0.25°/1 hour; ERA-Interim, ~0.75°/3 hour; MERRA2~0.5° × 0.625°/1 hour) from 2000 to 2018, and found that the IMERG product generally outperformed other datasets, except the Global Satellite Mapping of

Precipitation (GSMaP), which was adjusted at the daily scale by the gauge analysis (0.5°/daily) from the CPC (Mega et al., 2014). Therefore, we have compared the AIMERG with GSMaP, in case of the typhoon Chan-hom, which is coordinated with those in Figure 11. As shown in Fig. 14, though the spatial patterns of the GSMaP are similar with those of the AIMERG, the AIMERG provides much more details than GSMaP, especially over the northeastern Zhejiang Province. Meanwhile, AIMERG significantly overwhelms GSMaP in terms of both bias and random errors. For instance, GSMaP underestimates the precipitation (bias ~ -31%) twice as large as AIMERG (bias ~ -15%), and the random errors of GSMaP (MAE ~ 1.97 mm/hour, RMSE ~ 3.26 mm/hour) are also significantly larger than those of AIMERG (MAE ~ 1.44 mm/hour, RMSE ~ 2.50 mm/hour). Compared with the original IMERG in Figure 11, though the random errors of GSMaP are relatively larger, the bias of GSMaP (~ -31%) is significantly smaller than that of the original IMERG (~ -50%), which owes to the calibrations on the GSMaP at the daily scale. In future, we also encourage researchers to comprehensively evaluate and compare the AIMERG with other high resolution precipitation products at various spatio-temporal scales.

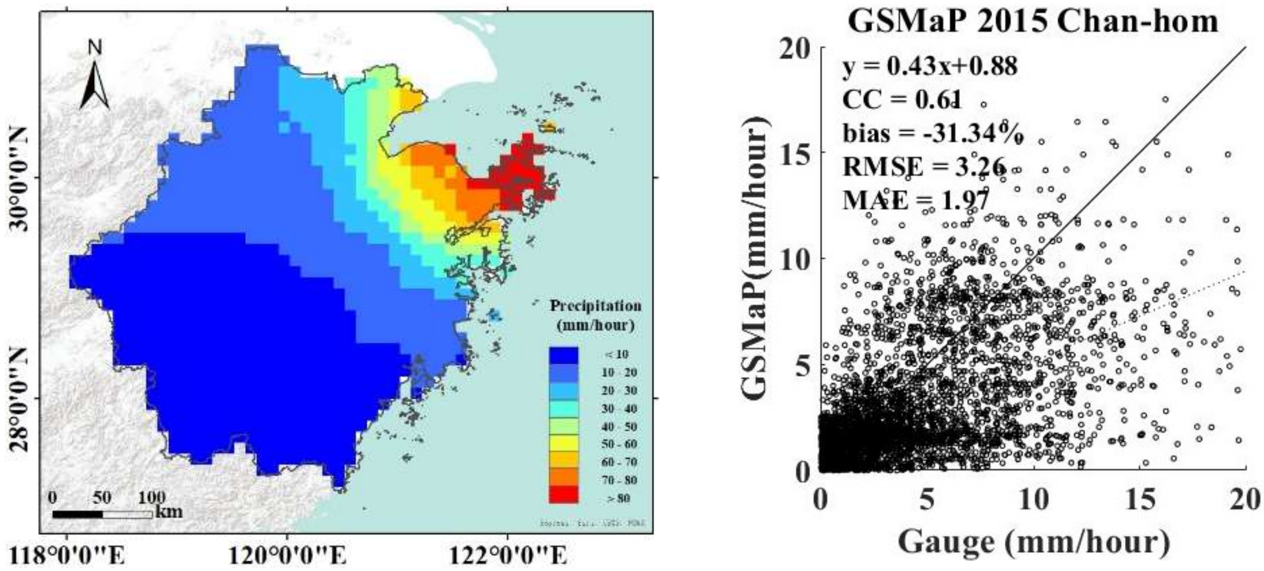

(a) (b)

Figure 14. The typhoon, Chan-hom, is selected as an example for assessing the quality of the Gauge adjusted GSMaP, occurred in the typical period 0 a.m., – 11 a.m., July, 11, 2015, in Zhejiang Province, which is coordinated with those in Figure 11. The background map used in this study was provided by Esri, USGS and NOAA (http://goto.arcgisonline.com/maps/World_Terrain_Base, last access: 17 January 2020).

The extent of the AIMERG could cover the Northern Eurasia, Middle East, Monsoon Asia, and Japan. This study mainly evaluated the AIMERG in the China Mainland, which calls for Asia wide evaluations in the future to assess both the algorithm and the corresponding precipitation product.

6. Data Availability

The AIMERG data record (0.1°/half-hourly, 2000-2015, Asia) is freely available at http://argi-basic.hihanlin.com:8000/d/d925fecf60/. Additionally, the AIMERG data is also freely accessible at https://doi.org/10.5281/zenodo.3609352 (for the period from 2000 to 2008) (Ma et al., 2020a) and http://doi.org/10.5281/zenodo.3609507 (for the period from 2009 to 2015) (Ma et al., 2020b).

7. Conclusions

As the milestone in the satellite-based precipitation measurement process, the TRMM and its successor GPM generate the most popular and the state-of-the-art satellite precipitation products for both water cycle related scientific researches and applications, TMPA (1998-present, 0.25°/3 hourly) and IMERG (2014-present, 0.1°/half-hourly), as well as the retrospective IMERG (2000-present, 0.1°/half-hourly) from GPM era to TRMM era. In this study, focusing on the potential drawbacks in generating IMERG and its recently updated retrospective IMERG (finished in July, 2019), which were only calibrated at monthly scale using limited ground observations, GPCC (1.0°/monthly), resulting the IMERG with large systematic bias and random errors, we introduce another daily gauge analysis product, APHRODITE (Last update October 5, 2018), to calibrate the IMERG at 0.25°/daily scale. Compared with GPCC, APHRODITE has inherently advantages with significantly larger numbers of ground observations and finer spatio-temporal resolutions (0.25°/daily), over the Asia.

We have proposed a new algorithm (Daily Spatio-Temporal Disaggregation Calibration Algorithm, DSTDCA) for calibrating IMERG at daily scale, and provided a new AIMERG precipitation dataset (0.1°/half-hourly, 2000-2015, Asia) (Ma et al., 2020a, b) with better quality, calibrated by APHRODITE at daily scale for the Asian applications. And the main conclusions include but not limited to: (1) the proposed daily calibration algorithm is effective in considering the advantages from both satellite-based precipitation estimates and the ground observations; (2) AIMERG performs better than IMERG at different spatio-temporal scales, in terms of both systematic biases and random errors, over the China Main land; and (3) APHRODITE demonstrates significant advantages than GPCC in calibrating the IMERG, especially over the mountainous regions with complex terrain, e.g., the Tibetan Plateau. Additionally, results of this study suggests that it is a promising and applicable daily calibration algorithm for GPM in generating the future IMERG in either operational scheme or retrospective manner.

Author Contributions

Dr. Ziqiang Ma designed and organized the manuscript. Drs. Jintao Xu, Siyu Zhu, Jun Yang and Yuanjian Yang prepared the related materials and run the models for generating AIMERG and the related assessments. Dr. Guoqiang Tang and Prof. Zhou Shi made contributions on the scientific framework of this study and discussed the interpretation of results. Prof. Yang Hong co-advised this study. All authors discussed the results and commented on the manuscript.

Competing interests

The authors declare they have no competing financial interests.

Acknowledgments

This study was financially supported by the Key R&D Program of Ministry of Science and Technology, China (Grant No. 2018YFC1506500); the National Natural Science Foundation of China (Grant No. 41901343); The Second Tibetan Plateau Scientific Expedition and Research (STEP) program (grant no. 2019QZKK0105); the China Postdoctoral Science Foundation (No. 2018M630037, and 2019T120021); the National Natural Science Foundation of China (Grant No. 91437214); the Open Fund of the State Key Laboratory of Remote Sensing Science, China (Grant No. OFSLRSS201909), the State Key Laboratory of Resources and Environmental Information System, China.

The contribution of the data providers is also greatly appreciated, including the Chinese Meteorological Data Sharing Service System (http://cdc.nmic.cn/home.do), the APHRODITE data provider (http://aphrodite.st.hirosaki-u.ac.jp/download/), and the IMERG data provider (https://pmm.nasa.gov/data-access/downloads/gpm).

References

Adler, R. F., Huffman, G. J., Chang, A., Ferraro, R., Xie, P., Janowiak, J., Rudolf, B., Schneider, U., Curtis, S., Bolvin, D., Gruber, A., Susskind, J., Arkin, P., and Nelkin, E.: The Version-2 Global Precipitation Climatology Project (GPCP) Monthly Precipitation Analysis (1979–Present), J. Hydrometeorol., 4, 1147–1167, https://doi.org/10.1175/1525-7541(2003)004<1147:TVGPCP>2.0.CO;2, 2003.

Adler, R.F., Sapiano, M., Huffman, G.J., Wang, J.-J., Gu, G., Bolvin, D.T., Chiu, L., Schneider, U., Becker, A., Nelkin, E.J., Xie, P., Ferraro, R., and Shin, D.-B.: The Global Precipitation Climatology Project (GPCP) Monthly Analysis (New Version 2.3) and a Review of 2017 Global Precipitation, Atmos., 9(4), 138, https://doi.org/10.3390/atmos9040138, 2018.

Beck, H. E., van Dijk, A. I. J. M., Levizzani, V., Schellekens, J., Miralles, D. G., Martens, B., and Roo, A. d.: MSWEP: 3-hourly 0.25° global gridded precipitation (1979–2015) by merging gauge, satellite, and reanalysis data, Hydrol. Earth Syst. Sci., 21, 589-615, https://doi.org/10.5194/hess-21-589-2017, 2017.

Beck, H. E., Wood, E. F., Pan, M., Fisher, C. K., Miralles, D. G., van Dijk, A. I. J. M., McVicar, T. R., and Adler, R. F.: MSWEP V2 Global 3-Hourly 0.1° Precipitation: Methodology and Quantitative Assessment, Bull. Amer. Meteorol. Soc., 100, 473-500, https://doi.org/10.1175/BAMS-D-17-0138.1, 2018.

Chen, M., Xie, P., Janowiak, J., and Arkin, P.: Global Land Precipitation: A 50-yr Monthly Analysis Based on Gauge Observations, J. Hydrometeorol., 3, 249-266, https://doi.org/10.1175/1525-7541(2002)003<0249:GLPAYM>2.0.CO;2, 2002.

Duncan, J. M. A., and Biggs, E. M.: Assessing the accuracy and applied use of satellite-derived precipitation estimates over Nepal, Appl. Geogr., 34, 626–638, https://doi.org/10.1016/j.apgeog.2012.04.001, 2014.

Ebert, E. E., Janowiak, J. E., and Kidd, C.: Comparison of Near-Real-Time Precipitation Estimates from Satellite Observations and Numerical Models, Bull. Amer. Meteorol. Soc., 88, 47-64, https://doi.org/10.1175/BAMS-88-1-47, 2007.

Hamada, A., Arakawa, O., and Yatagai, A.: An automated quality control method for daily rain-gauge data, Global Environmental Research, 15, 183-192, http://www.airies.or.jp/journal_15-2eng.html, 2011.

Hong, Y., Hsu, K.-L., Sorooshian, S., and Gao, X.: Precipitation Estimation from Remotely Sensed Imagery Using an Artificial Neural Network Cloud Classification System, J. Appl. Meteorol., 43, 1834-1853, https://doi.org/10.1175/JAM2173.1, 2004.

Huffman, G. J., Adler, R. F., Arkin, P., Chang, A., Ferraro, R., Gruber, A., Janowiak, J., McNab, A., Rudolf, B., and Schneider, U.: The Global Precipitation Climatology Project (GPCP) Version 1 data set, Bull. Am. Meteorol. Soc., 78, 5-20, https://doi.org/10.1175/1520-0477(1997)078<0005:TGPCPG>2.0.CO;2, 1997.

Huffman, G. J., Bolvin, D. T., Nelkin, E. J., Wolff, D. B., Adler, R. F., Gu, G., Hong, Y., Bowman, K. P., and Stocker, E. F.: The TRMM Multisatellite Precipitation Analysis (TMPA): Quasi-Global, Multiyear, Combined-Sensor Precipitation Estimates at Fine Scales, J. Hydrometeorol., 8, 38-55, https://doi.org/10.1175/JHM560.1, 2007.

Huffman, G. J., Bolvin, D. T., Braithwaite, D., Hsu, K., Joyce, R., Kidd, C., Nelkin, E. J., Sorooshian, S., Tan, J., and Xie, P.: NASA Global Precipitation Measurement (GPM) Integrated Multi-satellitE Retrievals for GPM (IMERG), Algorithm Theoretical Basis Document (ATBD) Version 06, NASA/GSFC, Greenbelt, MD, USA, 38pp., 2019a.

Huffman, G. J., E.F. Stocker, D.T. Bolvin, E.J. Nelkin, and Jackson Tan: GPM IMERG Final Precipitation L3 Half Hourly 0.1 degree x 0.1 degree V06, Greenbelt, MD, Goddard Earth Sciences Data and Information Services Center (GES DISC), https://doi.org/10.5067/GPM/IMERG/3B-HH/06, 2019b.

Joyce, R. J., Janowiak, J. E., Arkin, P. A., and Xie, P.: CMORPH: A Method that Produces Global Precipitation Estimates from Passive Microwave and Infrared Data at High Spatial and Temporal Resolution, J. Hydrometeorol., 5, 487-503, https://doi.org/10.1175/1525-7541(2004)005<0487:CAMTPG>2.0.CO;2, 2004.

Lu, H., Ding, L., Ma, Z., Li, H., Lu, T., Su, M., and Xu, J.: Spatiotemporal Assessments on the Satellite-Based Precipitation Products From Fengyun and GPM Over the Yunnan-Kweichow Plateau, China, Earth Space Sci., 7, e2019EA000857, https://doi.org/10.1029/2019EA000857, 2020.

Mega, T., Ushio, T., Kubota, T., Kachi, M., Aonashi, K., and Shige, S.: Gauge adjusted global satellite mapping of precipitation (GSMaP_Gauge), in: 2014 XXXIth URSI General Assembly and Scientific Symposium (URSI GASS), Beijing, China, 17-23 August 2014,1–4. 2014.

Ménégoz, M., Gallée, H., and Jacobi, H. W.: Precipitation and snow cover in the Himalaya: from reanalysis to regional climate simulations, Hydrol. Earth Syst. Sci., 17, 3921–3936, https://doi.org/10.5194/hess-17-3921-2013, 2013.

Ma, Z., Jin, X., Zhu, S., Tang, G., Yang, Y., Shi, Z., and Hong, Y.: AIMERG: a new Asian precipitation dataset (0.1°/half-hourly, 2000-2008) by calibrating GPM IMERG at daily scale using APHRODITE [Data set], Zenodo, https://doi.org/10.5281/zenodo.3609352, 2020.

Ma, Z., Jin, X., Zhu, S., Tang, G., Yang, Y., Shi, Z., and Hong, Y.: AIMERG: a new Asian precipitation dataset (0.1°/half-hourly, 2009-2015) by calibrating GPM IMERG at daily scale using APHRODITE [Data set], Zenodo, https://doi.org/10.5281/zenodo.3609507, 2020.

Ma, Z., Shi, Z., Zhou, Y., Xu, J., Yu, W., and Yang, Y.: A spatial data mining algorithm for downscaling TMPA 3B43 V7 data over the Qinghai–Tibet Plateau with the effects of systematic anomalies removed, Remote Sens. Environ., 200, 378-395, https://doi.org/10.1016/j.rse.2017.08.023, 2017.

Matsuura, K., and Willmott C. J.: Terrestrial precipitation: 1900–2008 gridded monthly time series (version 2.01), Center for Climatic Research Department of Geography Center for Climatic Research, University of Delaware, http://climate.geog.udel.edu/~climate/html_pages/Global2_Ts_2009/README.global_p_ts_2009.html, 2009.

Mitchell, T. D., and Jones, P. D.: An improved method of constructing a database of monthly climate observations and associated high-resolution grids, Int. J. Climatol., 25, 693-712, https://doi.org/10.1002/joc.1181, 2005.

Rajeevan, M., and Bhate, J.: A high resolution daily gridded rainfall dataset (1971–2005) for mesoscale meteorological studies, Curr. Sci., 96, 558-562, https://www.jstor.org/stable/24105470, 2009.

Rozante, J. R., Moreira, D. S., Goncalves, L.G., and Vila, D. A.: Combining TRMM and surface observations of precipitation: technique and validation over South America, Wea. Forecasting, 25, 885-894, https://doi.org/10.1175/2010WAF2222325.1, 2010.

Schneider, U., Fuchs, T., Meyer-Christoffer, A., and Rudolf, B.: Global precipitation analysis products of the GPCC. Global Precipitation Climatology Centre, DWD, 13 pp., 2008

Schneider, U., Becker, A., Finger, P., Meyer-Christoffer, A., Ziese, M., and Rudolf, B.: GPCC's new land surface precipitation climatology based on quality-controlled in situ data and its role in quantifying the global water cycle, Theor. Appl. Climatol., 115, 15-40, https://doi.org/10.1007/s00704-013-0860-x, 2014.

Schneider, U., P. Finger, A. Meyer-Christoffer, M. Ziese, A. Becker: Global Precipitation Analysis Products of the GPCC. GPCC Internet Publication, DWD, 17 pp., 2018

Shen, Y., Feng, M. N. Zhang, H. Z. and Gao, X.: Interpolation methods of China daily precipitation data [in Chinese], J. Appl. Meteorol. Sci., 21, 279–286, https://doi.org/10.11898/1001-7313.20100303, 2010.

Shen, Y., Zhao, P., Pan, Y., and Yu, J.: A high spatiotemporal gauge-satellite merged precipitation analysis over China, J. Geophys. Res. Atmos., 119, https://doi.org/10.1002/2013JD020686, 2014.

Sorooshian, S., Hsu, K.-L., Gao, X., Gupta, H. V., Imam, B., and Braithwaite, D.: Evaluation of PERSIANN System Satellite-Based Estimates of Tropical Rainfall, Bull. Amer. Meteorol. Soc., 81, 2035-2046, https://doi.org/10.1175/1520-0477(2000)081<2035:EOPSSE>2.3.CO;2, 2000.

Sunilkumar, K., Yatagai, A., and Masuda, M.: Preliminary evaluation of GPM-IMERG rainfall estimates over three distinct climate zones with APHRODITE. Earth Space Sci., 6, 1321– 1335. https://doi.org/10.1029/2018EA000503, 2019.

Tang, G., Ma, Y., Long, D., Zhong, L., and Hong, Y.: Evaluation of GPM Day-1 IMERG and TMPA Version-7 legacy products over Mainland China at multiple spatiotemporal scales, J. Hydrol., 533, 152-167, https://doi.org/10.1016/j.jhydrol.2015.12.008, 2016.

Tang, G., Clark, M. P., Papalexiou, S. M., Ma, Z., and Hong, Y.: Have satellite precipitation products improved over last two decades? A comprehensive comparison of GPM IMERG with nine satellite and reanalysis datasets, Remote Sens. Environ., 240, 111697, https://doi.org/10.1016/j.rse.2020.111697, 2020.

Xie, P., and Xiong, A.: A conceptual model for constructing high-resolution gauge-satellite merged precipitation analyses, J. Geophys. Res. Atmos., 116, https://doi.org/10.1029/2011JD016118, 2011.

Xu, J., Ma, Z., Tang, G., Ji, Q., Min, X., Wan, W., and Shi, Z.: Quantitative Evaluations and Error Source Analysis of Fengyun-2-Based and GPM-Based Precipitation Products over Mainland China in Summer, 2018, Remote Sens., 11, https://doi.org/10.3390/rs11242992, 2019.

Yatagai, A., Xie, P., and Kitoh, A.: Utilization of a New Gauge-based Daily Precipitation Dataset over Monsoon Asia for Validation of the Daily Precipitation Climatology Simulated by the MRI/JMA 20-km-mesh AGCM, SOLA, 1, 193-196, https://doi.org/10.2151/sola.2005-050, 2005.

Yatagai, A., Kamiguchi, K., Arakawa, O., Hamada, A., Yasutomi, N., and Kitoh, A.: APHRODITE: Constructing a Long-Term Daily Gridded Precipitation Dataset for Asia Based on a Dense Network of Rain Gauges, Bull. Amer. Meteorol. Soc., 93, 1401-1415, https://doi.org/10.1175/BAMS-D-11-00122.1, 2012.

Yong, B., Ren, L.-L., Hong, Y., Wang, J.-H., Gourley, J. J., Jiang, S.-H., Chen, X., and Wang, W.: Hydrologic evaluation of Multisatellite Precipitation Analysis standard precipitation products in basins beyond its inclined latitude band: A case study in Laohahe basin, China, Water Resour. Res., 46, https://doi.org/10.1029/2009WR008965, 2010.

Appendix A: Acronyms with definitions used in this study.

AIMERG	Asian precipitation dataset by calibrating GPM IMERG at daily scale using APHRODITE
APHRODITE	Asian Precipitation Highly Resolved Observational Data Integration Towards Evaluation of Water Resources
ATBD	Algorithm Theoretical Basis Document
BIAS	Relative Bias
CC	Correlation Coefficient
CHIRPS	Climate Hazards group Infrared Precipitation with Stations
CLIMAT	Monthly Climatological Data
CMA	Chinese Meteorological Administration
CMORPH	Climate Prediction Center (CPC) MORPHing technique
CPC	Climate Prediction Center
CSI	Critical Success Index
DSTDCA	Daily Spatio-Temporal Disaggregation Calibration Algorithm
DWD	Deutscher Wetterdienst
ERA5	Fifth generation of ECMWF atmospheric reanalyses of the global climate
ERA-Interim	ECMWF ReAnalysis Interim
FAR	False Alarm Ratio
GEWEX	Global Energy and Water Exchange
GPCC	Global Precipitation Climatology Centre

GPM	Global Precipitation Measurement
GSMaP	Gauge-adjusted Global Satellite Mapping of Precipitation V7
GTS	Global Telecommunications System
IMERG	Integrated Multi-satellitE Retrievals for GPM
IR	Infrared
ME	Mean Error
MERRA2	The Modern-Era Retrospective Analysis for Research and Applications, Version 2
MW	Microwave
NHMs	National hydrological and meteorological services
NMIC	National Meteorological Information Center
OI	Optimal Interpolation
PDF	Probability Density Function
PERSIANN	Precipitation Estimation from Remotely Sensed Information using Artificial Neural Networks
PERSIANN-CCS	Precipitation Estimation from Remotely Sensed Information using Artificial Neural Networks-Cloud Classification System
PERSIANN-CDR	PERSIANN-Climate Data Record
PMW	Passive Microwave
POD	Probability of Detection

QC	Quality Control
RMSD	Root-mean-square Deviation
RMSE	Root Mean Square Error
SG	Satellite-Gauge
SM2RAIN	Soil Moisture to RAIN based on ESA Climate Change Initiative (CCI)
SYNOP	Synoptic Weather Report
TMPA	TRMM Multi-satellite Precipitation Analysis
TRMM 3B42	Tropical Rainfall Measuring Mission Multi-satellite Precipitation Analysis 3B42 V7